United States
Environmental Protection
Agency

EPA-600/R-01-054
August 2001

Research and Development

Chlorine Absorption In S(IV) Solutions

Prepared for

Office of Research and Development

Prepared by

National Risk Management
Research Laboratory
Research Triangle Park, NC 27711

Foreword

The U.S. Environmental Protection Agency is charged by Congress with protecting the Nation's land, air, and water resources. Under a mandate of national environmental laws, the Agency strives to formulate and implement actions leading to a compatible balance between human activities and the ability of natural systems to support and nurture life. To meet this mandate, EPA's research program is providing data and technical support for solving environmental problems today and building a science knowledge base necessary to manage our ecological resources wisely, understand how pollutants affect our health, and prevent or reduce environmental risks in the future.

The National Risk Management Research Laboratory (NRMRL) is the Agency's center for investigation of technological and management approaches for preventing and reducing risks from pollution that threaten human health and the environment. The focus of the Laboratory's research program is on methods and their cost-effectiveness for prevention and control of pollution to air, land, water, and subsurface resources, protection of water quality in public water systems; remediation of contaminated sites, sediments and ground water; prevention and control of indoor air pollution; and restoration of ecosystems. NRMRL collaborates with both public and private sector partners to foster technologies that reduce the cost of compliance and to anticipate emerging problems. NRMRL's research provides solutions to environmental problems by: developing and promoting technologies that protect and improve the environment; advancing scientific and engineering information to support regulatory and policy decisions; and providing the technical support and information transfer to ensure implementation of environmental regulations and strategies at the national, state, and community levels.

This publication has been produced as part of the Laboratory's strategic long-term research plan. It is published and made available by EPA's Office of Research and Development to assist the user community and to link researchers with their clients.

E. Timothy Oppelt, Director
National Risk Management Research Laboratory

EPA REVIEW NOTICE

EPA-600/R-01-054
August 2001

Chlorine Absorption in S(IV) Solutions

By

Sharmistha Roy and Gary T. Rochelle
Department of Chemical Engineering
The University of Texas at Austin
Austin, TX 78712

U.S. EPA Cooperative Agreement CR 827608-01-1

U.S. EPA Project Officer

Theodore G. Brna
National Risk Management Research Laboratory
Air Pollution Prevention and Control Division
Research Triangle Park, NC 27711

Prepared for:

United States Environmental Protection Agency
Office of Research and Development
Washington DC 20460

Abstract

The rate of chlorine (Cl_2) absorption into aqueous sulfite/bisulfite [S(IV)] solutions was measured at ambient temperature using a highly characterized stirred cell reactor. The reactor media were 0 to 10 mM S(IV) with pH ranging from 3.5 to 8.5. Experiments were performed using 20 to 300 ppm Cl_2 in nitrogen (N_2). Chlorine absorption was modeled using the theory of mass transfer with chemical reaction. Chlorine reacts quickly with S(IV) to form chloride and sulfate. Chlorine absorption is enhanced by increasing pH and S(IV) concentration. The rate constant for the reaction of chlorine with S(IV) was too rapid to be precisely measured using the existing stirred cell reactor, due to mass transfer limitations. However, the most probable value of the rate constant was determined to be 2×10^9 L/mol-s.

These results are relevant in the simultaneous removal of chlorine, sulfur dioxide (SO_2), and elemental mercury (Hg) from flue gas. The developed model shows that good removal of both chlorine and mercury should be possible with the injection of 1 to 10 ppm chlorine to an existing limestone slurry scrubber. These results may also be applicable to scrubber design for removal of chlorine in the pulp and paper and other industries.

Contents

Tables

Figures

Nomenclature

A	gas/liquid contact area (m^2)
A^-	generic anion
C_{Cl_2}	concentration of chlorine in liquid (mol/L = M = kmol/m^3)
$[Cl^-]$	concentration of chloride in liquid (M)
D_{Cl_2}	diffusion coefficient for chlorine in water (m^2/s)
D_{Hg}	diffusion coefficient for mercury in water (m^2/s)
$D_{S(IV)}$	diffusion coefficient for S(IV) in water (m^2/s)
E	enhancement factor (dimensionless)
FC	mass flow controller
Φ	reactant stoichiometric coefficient (dimensionless)
G	gas flow rate to reactor (m^3/s)
HA	generic acid
H_{Cl_2}	Henry's law constant for chlorine (atm-m^3/kmol)
H_{Hg}	Henry's law constant for mercury (atm-m^3/kmol)
IMS	ion mobility spectrometry
K	equilibrium constant
k_g	individual gas film mass transfer coefficient (kmol/s-atm-m^2)
k^o_{L,Cl_2}	individual physical liquid film mass transfer coefficient for chlorine (m/s)
K_{OG}	overall gas phase mass transfer coefficient (kmol/s-atm-m^2)
$k_{1,H2O}$	first order rate constant for chlorine hydrolysis reaction (s^{-1})
$k_{2,buf}$	second order rate constant for chlorine/buffer reaction (L/mol-s)
$k_{2,Hg}$	second order rate constant for mercury/chlorine reaction (L/mol-s)
$k_{2,S(IV)}$	second order rate constant for chlorine/S(IV) reaction (L/mol-s)
$k_{2,OH}$	second order rate constant for chlorine/hydroxide reaction (L/mol-s)
N_{Cl_2}	flux of chlorine (kmol/m^2-s)
N_g	number of gas phase mass transfer units, defined as k_gA/G (dimensionless)
n_g	gas phase agitation rate (rpm)
n_L	liquid phase agitation rate (rpm)
P_{Cl_2}	partial pressure of chlorine (atm)
$P^*_{Cl_2,b}$	partial pressure of chlorine in equilibrium with chlorine in bulk liquid (atm)
pK_a	negative logarithm of acid dissociation constant
R	gas constant (8.205 x 10^{-5} m^3-atm/mol-°C)
t	time (s)
T	temperature (°C)

V	reactor volume (m^3)
y_{Hg}	mole fraction of mercury in the gas phase (dimensionless)

Subscripts

b	in bulk
i	at gas/liquid interface
in	inlet
init	initial
out	outlet
T	total

1. Introduction

Mercury (Hg) pollution is an important problem because of its behavior in the environment (bioaccumulation) and the potential for deleterious health effects. Roughly 85% of anthropogenic mercury emissions are from combustion sources (Keating et al., 1997). The flue gas from these sources contains sulfur dioxide (SO_2) and hydrogen chloride (HCl) at much higher concentrations than the mercury compounds. Aqueous scrubbing is currently used to remove SO_2 and HCl from these flue gases. It should be possible to remove Hg by conventional aqueous scrubbing technologies with the addition of reagents to produce chlorine, which will oxidize the Hg to a more soluble form through reaction in the mass transfer boundary layer. Some researchers, such as Zhao (1997) and Livengood and Mendelsohn (1997), have had success in removing Hg via reactions with chlorine compounds. Mercury reacts with chlorine to form mercuric chloride, $HgCl_2$, which is very soluble (Ernst et al., 1997) and can thus be easily removed through aqueous scrubbing. Figure 1-1 depicts the process in a limestone slurry scrubber.

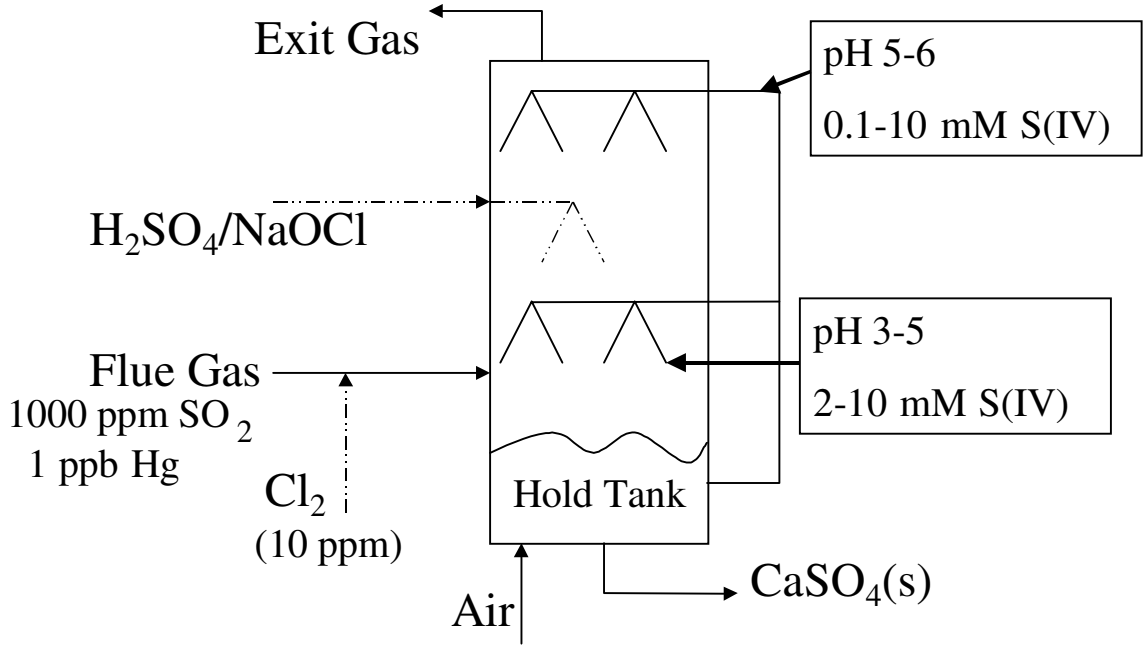

Figure 1-1. Chlorine injection for Hg removal in limestone slurry scrubbing

In the proposed technology, either hypochlorite solution will be sprayed into the scrubber to generate chlorine in-situ or chlorine gas (< 10 ppm) will be directly injected into the gaseous feed as shown in Figure 1-1. The chlorine cannot be introduced with the bulk solution. If an oxidant were put in the bulk solution, it would be completely depleted by reaction with dissolved S(IV). Hypochlorite will release Cl_2 upon acidification by absorption of SO_2 and HCl or by addition of sulfuric acid. The Cl_2 should react with elemental Hg in the solution at the gas/liquid interface and should greatly enhance the rate of absorption of Hg. The mercury will be oxidized and absorbed into the scrubber solution. The chlorine will also react at the gas/liquid interface with any elemental Hg formed by sulfite reduction of $HgCl_2$ in the bulk solution.

The success of this approach requires that the mercury react with the chlorine before it gets reduced by the dissolved SO_2 present as S(IV). S(IV) represents sulfur in the +4 oxidation state (sulfite and bisulfite). Therefore, the kinetics of the reaction between chlorine and S(IV) need to be quantified to ensure that the chlorine will be available to react with the Hg. Measuring the reaction rate of chlorine with S(IV) is the topic of this report.

2. Conclusions

The rate constant for the Cl_2/S(IV) reaction was too rapid to be precisely measured using the stirred cell reactor, due to mass transfer limitations. However, the most probable value for the rate constant was determined to be 2×10^9 L/mol-s. At low S(IV), the chlorine absorption was limited by the buffer-enhanced hydrolysis reaction. At moderate S(IV), it was limited by diffusion of S(IV) from the bulk solution to the interface. At high S(IV), the absorption was limited by diffusion of chlorine from the bulk gas to the interface.

Chlorine injection to enhance mercury removal may be a feasible process. In a typical limestone slurry scrubber, chlorine absorption will be gas film controlled because of the rapid Cl_2/S(IV) reaction rate. Thus, 99 to 99.99% chlorine removal will be achieved in typical scrubbers. Also, there will be enough chlorine at the interface to react with mercury. The model shows that only 1 ppm chlorine is needed to get 99% mercury removal.

The succinate buffer enhances chlorine absorption. However, lowering the succinate buffer concentration did not aid in extracting kinetics because there is not much of a range between the chlorine flux due to absorption in water and the maximum flux resulting from complete gas film control. Therefore, extracting kinetics for the S(IV) reaction will always be difficult in the existing apparatus. On one end, absorption is limited by the chlorine hydrolysis reaction, and on the other end, it is limited by gas film control in the stirred cell contactor.

Chloride does not affect chlorine absorption in S(IV) since the chlorine/S(IV) reaction is irreversible. Oxygen does not affect chlorine absorption in S(IV) either, nor does it seem to catalyze S(IV) depletion at the ranges investigated.

3. Recommendations

In order to accurately predict mercury and chlorine removal in a scrubber, a better model with precise kinetics is needed. The Cl_2/S(IV) reaction rate needs to be precisely measured in a gas/liquid contactor with higher mass transfer coefficients. Furthermore, this reaction rate should be measured at 55°C to simulate a typical limestone slurry scrubber.

Simultaneous absorption of mercury and chlorine must be measured and modeled to obtain a precise value for $k_{2,Hg}$. These experiments should also be done at 55°C. Simultaneous absorption of Hg, Cl_2, and SO_2 should also be studied. Furthermore, in order to completely simulate flue gas, CO_2, NO_x, and O_2 should be added to the inlet gas.

Results have shown that chloride does not affect chlorine absorption. However, experiments were not done in sodium chloride solutions higher than 0.02 M. Limestone slurry may have 1 M Cl^-. Thus, absorption into 1 M chloride must be quantified.

4. Literature Review

4.1 Mercury removal with chlorine

Previous researchers have performed screening experiments on mercury removal through reaction with chlorine oxidants. Zhao (1999) investigated Hg absorption in hypochlorite/chloride solutions and showed that low pH, high temperature, and high Cl^- concentration favored Hg absorption. In aqueous hypochlorite solution, the distribution of OCl^-, HOCl, and Cl^- depends on solution pH and $[Cl^-]$. Since lower pH results in higher Hg removal, it is probable that free Cl_2 is the active species that reacts with Hg. The activity of free Cl_2 can be obtained from the following two equilibria:

$$HOCl \xleftrightarrow{K_1} H^+ + OCl^- \quad (4\text{-}1)$$

$$Cl_2 + H_2O \xleftrightarrow{K_2} HOCl + Cl^- + H^+ \quad (4\text{-}2)$$

Thus, at low pH (high H^+) and high Cl^-, the formation of Cl_2 is favored. The chlorine reacts with the Hg to form $HgCl_2$ in an apparent overall second order reaction and greatly enhances the rate of Hg absorption. The rate constant was obtained from modeling the Hg absorption using surface renewal theory for mass transfer with fast chemical reaction in the boundary layer. The rate constant measured by Zhao in hypochlorite solutions at pH 9 to 11 was 1.7×10^{15} L/mol-s at 25°C and 1.4×10^{17} L/mol-s at 55°C. Furthermore, preliminary experiments with simultaneous absorption of chlorine and Hg have demonstrated that 1 to 10 ppm of chlorine can be effective in removing 0.1 ppm Hg (Zhao, 1999).

Fedorovskaya et al. (1979) said that Hg removal with an acidic chlorine-containing solution can be represented by two mechanisms: (1) chlorine from the solution is swept into the gas phase where it oxidizes the Hg and (2) Hg diffuses from the gas into the solution and reacts with the chlorine. Their experiments showed that when the chlorine/mercury ratio is less than 20:1, mercurous chloride is the primary product formed. At ratios greater than 20:1, the oxidation of Hg with chlorine yields mercuric chloride. This reaction takes place rapidly (in 1-2 seconds). Fedorovskaya et al. (1979) also showed that oxidation of Hg can occur in alkaline medium in the presence of hypochlorite/chloride. They found that the oxidation of Hg is still fast under these conditions, but the reaction is twice as fast in acid because of higher oxidizing potentials in acid.

Mercury is also known to react with Cl_2 in the gas phase with a reaction rate constant of 2×10^5 L/mol-s at 20°C (Hall, 1992). Hall's experiments showed that the reaction rate was relatively independent of temperature from 20°C to 700°C. Thus, the apparent activation energy is probably not greater than 10 kJ/mol. Mercury removal via gas phase reaction with chlorine can be quantified using this rate constant and a typical commercial gas phase residence time of 2 seconds. If the gas inlet were 1 ppb Hg and 10 ppm chlorine, 0.84 ppb Hg would exit the scrubber. Therefore, gas phase reaction with chlorine is not enough to remove Hg.

4.2 Chlorine absorption in aqueous solutions

There are several reactions which contribute to chlorine absorption in aqueous solutions. At a pH of 3 to 10.5 (with no S(IV) present), chlorine hydrolysis to form hypochlorous acid and hydrochloric acid is the dominant reaction controlling chlorine absorption (Spalding, 1962). This reaction is relatively slow, $k_{1,H2O} = 15.4\ s^{-1}$ at 25°C (Brian et al., 1966). Under typical limestone slurry scrubber conditions, if 10 ppm Cl_2 were injected into the gaseous feed, 8.5 ppm Cl_2 would exit if chlorine absorption in water were the only reaction enhancing chlorine absorption. Therefore, the chlorine hydrolysis reaction alone will not cause the chlorine at the gas-liquid interface to be depleted.

Chlorine hydrolysis can be enhanced by the presence of buffer anions (Wang and Maregerum, 1994; Lifshitz and Perlmutter-Hayman, 1962). The following overall reaction occurs:

$$Cl_2 + H_2O + A^- \leftrightarrow HOCl + Cl^- + HA \qquad (4\text{-}3)$$

The kinetics of this reaction have been studied for the following anions (A^-): acetate, chloroacetate, formate, and phosphate (Lifshitz and Perlmutter-Hayman, 1962).

At a pH greater than 10.5, the chlorine/hydroxide reaction shown below is the dominant reaction:

$$Cl_2 + 2OH^- \rightarrow Cl^- + OCl^- + H_2O \qquad (4\text{-}4)$$

(Spalding, 1962). This reaction is relatively fast, $k_{2,OH} = 1.57 \times 10^9$ L/mol-s (Ashour et al., 1996); thus, at high pH, there will be no chlorine at the gas/liquid interface.

Chlorine can also react with sulfite to form chloride and sulfate (Askew and Morisani, 1989; Gordon et al., 1990).

$$Cl_2 + H_2O + SO_3^{-2} \rightarrow 2Cl^- + SO_4^{-2} + 2H^+ \qquad (4\text{-}5)$$

This reaction has not been studied much; thus, the kinetics have not been quantified.

4.3 Reactions of S(IV) with chlorine oxidants

Even though the Cl_2/S(IV) reaction kinetics have not been studied, researchers have investigated S(IV) reactions with various chlorine oxidants. Hypochlorous acid (HOCl) and hypochlorite (OCl^-) can react with sulfite (SO_3^{-2}) (Fogelman et al., 1989). Hypochlorous acid reacts as follows:

$$HOCl + SO_3^{-2} \rightarrow OH^- + ClSO_3^- \qquad (4\text{-}6)$$

$$ClSO_3^- + H_2O \rightarrow Cl^- + SO_4^{-2} + 2H^+ \qquad (4\text{-}7)$$

The first reaction has a rate constant of 7.6×10^8 L/mol-s at 25°C and ionic strength of 0.5, but the rate limiting step is the second reaction, which has a rate constant of $270\ s^{-1}$.

Hypochlorite reacts with sulfite as shown below:

$$OCl^- + SO_3^{-2} \rightarrow Cl^- + SO_4^{-2} \qquad (4\text{-}8)$$

The rate of oxidation of sulfite with HOCl is more than four orders of magnitude faster than the rate with OCl^-. A shift in mechanism is proposed to account for the huge increase in reactivity (Fogelman et al., 1989).

Suzuki and Gordon (1978) investigated the reaction of chlorine dioxide (ClO_2) with S(IV) in basic solutions, where S(IV) represents sulfur in the +4 oxidation state (primarily sulfite and bisulfite). The overall stoichiometry is:

$$nClO_2 + mS(IV) \rightarrow pClO_2^- + qClO_3^- + rCl^- + mSO_4^{-2} \qquad (4\text{-}9)$$

The coefficients n, m, p, q, and r depend on both the pH and the specific buffer solution used.

Reactions of S(IV) with chlorine oxidants are important in water and wastewater treatment. Here, sulfite is used to deplete residual chlorine (such as chloramines and chloropeptides) which remains after water disinfection using chlorine. A monochloropeptide reacts with sulfite as shown (Jensen and Helz, 1998).

$$ClNH\text{-peptide} + SO_3^{-2} + 2H_2O \rightarrow NH_2\text{-peptide} + Cl^- + SO_4^{-2} + H_3O^+ \qquad (4\text{-}10)$$

Jensen and Helz (1998) say that usually bisulfite (HSO_3^-) is a much poorer reducing agent than sulfite (SO_3^{-2}). So, reaction rates of chlorine oxidants are much faster with sulfite than with bisulfite.

Sulfite is also used to remove chlorite (which can result from using chlorine dioxide as a disinfectant) from treated water. The reaction is (Gordon et al., 1990):

$$ClO_2^- + 2SO_3^{-2} \rightarrow Cl^- + 2SO_4^{-2} \qquad (4\text{-}11)$$

5. Mass Transfer with Chemical Reaction

Chlorine absorption into S(IV) solutions occurs by mass transfer with simultaneous chemical reaction. Chlorine must first diffuse from the bulk gas to the gas liquid interface with the flux (N_{Cl_2}) given by:

$$N_{Cl_2} = k_g (P_{Cl_{2,b}} - P_{Cl_{2,i}}) \tag{5-1}$$

Then, chlorine absorption into the liquid occurs by mass transfer with fast chemical reaction in the boundary layer with the same flux:

$$N_{Cl_2} = \frac{E k^o_{L,Cl_2} (P_{Cl_2,i} - P^*_{Cl_2,b})}{H_{Cl_2}} \tag{5-2}$$

According to surface renewal theory (Danckwerts, 1970), the enhancement factor (E) can be expressed as (Critchfield, 1988; Shen, 1997; Zhao, 1997):

$$E = \sqrt{1 + \frac{D_{Cl_2}}{k^{o2}_L}\left(k_{1,H_2O} + k_{2,buf}[\text{buffer}]_i + k_{2,OH}[OH^-]_i + k_{2,S(IV)}[S(IV)]_i\right)} \tag{5-3}$$

which incorporates the reactions which contribute to chlorine absorption. If the chlorine/S(IV) reaction is the dominant reaction and equilibrium effects are negligible, then the flux expression simplifies to:

$$N_{Cl_2} = E k^o_{L,Cl_2} \frac{P_{Cl_{2i}}}{H_{Cl_2}} = \frac{P_{Cl_{2i}}}{H_{Cl_2}} \sqrt{D_{Cl_2} k_{2,S(IV)} [S(IV)]_i} \tag{5-4}$$

The enhancement factor expression is derived assuming that the chlorine/S(IV) reaction is first order in chlorine and first order in S(IV). If this model is correct, the extracted rate constant, $k_{2,S(IV)}$, can be used to extrapolate chlorine removal at low chlorine concentrations. The corresponding rate expression is:

$$\text{reaction rate} = k_{2,S(IV)} [Cl_2][S(IV)] \tag{5-5}$$

The concentrations, physical properties (diffusivity, D, and Henry's law constant, H) and rate constants for the water and hydroxide reactions are known. At 25°C, the Henry's law constant for chlorine, H_{Cl_2}, was taken to be 16.7 atm-m^3/kmol (Brian et al., 1966), and the diffusion coefficient for chlorine through water, D_{Cl_2}, was taken to be 1.48 x 10^{-9} m^2/s (Spalding, 1962). The chlorine flux was determined experimentally from the gas phase material balance. Thus, the only unknown is the rate constant for the chlorine/S(IV) reaction. This rate constant, $k_{2,S(IV)}$, can be calculated by substituting the enhancement factor into the flux equation (5-2).

The interfacial liquid S(IV) concentration is obtained by assuming that Cl_2 reacts with S(IV) at the gas/liquid interface.

$$N_{Cl2} = \Phi N_{S(IV)} = \Phi k^{o}_{L,\,S(IV)}([S(IV)]_b - [S(IV)]_i) \tag{5-6}$$

$$[S(IV)]_i = [S(IV)]_b - \frac{N_{Cl_2}}{\Phi k^{o}_{L,S(IV)}} \tag{5-7}$$

Φ represents the stoichiometric relationship between the reactants. For example, in the reaction $Cl_2 + 2OH^- \rightarrow Cl^- + OCl^- + H_2O$, $\Phi = ½$ since 1 mol of Cl_2 reacts with 2 mol of OH^-.

The rate constant can only be extracted if mass transfer does not limit the chlorine absorption. When the S(IV) concentration is high relative to the chlorine concentration, the chlorine flux is limited by the resistance in the gas phase, and the flux from Equation 5-1 simplifies to:

$$N_{Cl_2} = k_g P_{Cl_{2,b}} \tag{5-8}$$

Under these conditions, there is essentially no chlorine at the interface since all the chlorine reacts with S(IV) as soon as the chlorine reaches the interface. Thus, the chlorine absorption only depends on how fast the chlorine diffuses from the bulk gas to the gas/liquid interface, not on the kinetics.

When the chlorine concentration is high relative to the S(IV) concentration, the flux is limited by S(IV) depletion at the interface. This means that there is essentially no S(IV) at the interface since whatever S(IV) diffuses to the interface is readily depleted through reaction with chlorine. Under these conditions, the flux in Equation 5-6 simplifies to:

$$N_{Cl2} = \Phi N_{S(IV)} = \Phi k^{o}_{L,\,S(IV)}[S(IV)]_b \tag{5-9}$$

showing that the flux of chlorine is linear with the bulk S(IV) concentration.

The fraction gas film resistance is a parameter used in analyzing some of the data. The fraction gas film resistance is directly related to reaction kinetics:

$$\frac{K_{OG}}{k_g} = \frac{1}{1 + \dfrac{k_g H_{Cl_2}}{E k^{o}_{L,Cl_2}}} = \text{fraction gas film resistance} \tag{5-10}$$

As the enhancement factor (E) increases, which corresponds to fast reaction rates, the total resistance to mass transfer ($1/K_{OG}$) becomes limited by gas film resistance ($1/k_g$). Under these conditions, the fraction gas film resistance (5-10) approaches unity and becomes independent of reaction kinetics. Thus, data which approach gas film resistance cannot be used for extracting kinetics. For these data, the gas film mass transfer coefficient (as opposed to kinetics) is being measured.

6. Experimental Apparatus and Methods

All chlorine absorption experiments were performed at ambient temperature (22 to 25°C) in the well-characterized stirred cell contactor with Teflon surfaces shown in Figure 6-1 (Zhao and Rochelle, 1999; Zhao, 1997). Teflon tubing, fittings, and valves were used for all the connections. Mass flow controllers are labeled as "FC."

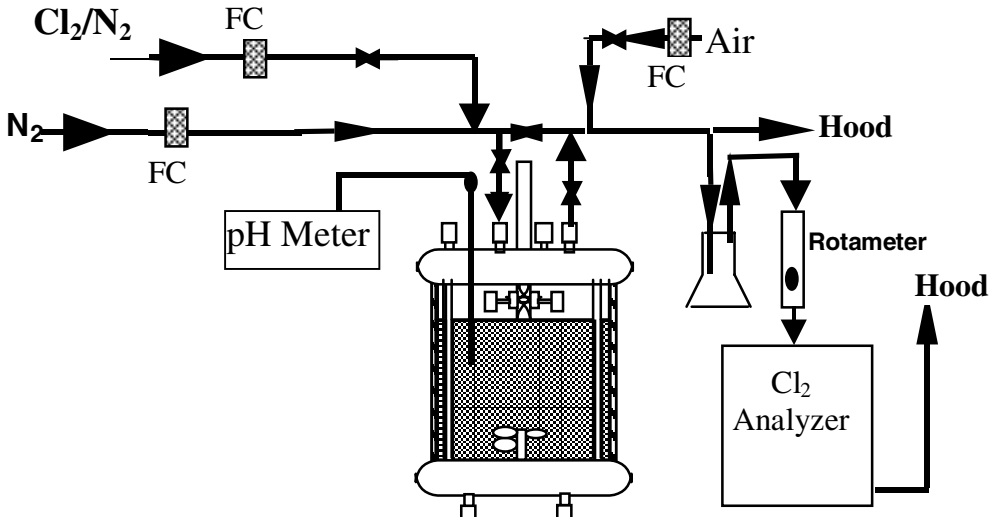

Figure 6-1. Stirred cell reactor apparatus

6.1 Description of stirred cell reactor apparatus

The stirred cell contactor allowed gas/liquid contact, for which mass transfer properties were known or measured, at a known interfacial area (A) of 8.1 x 10^{-3} m^2. The cylindrical reactor had a 0.01 m inner diameter and 0.016 m height. The reactor vessel consisted of a thick glass cylinder with Teflon-coated 316 stainless steel plates sealed to the top and bottom by thick gasket clamps. Four equally-spaced, Teflon-coated, 316 stainless steel baffles were welded to the bottom plate. The length of the baffles was long enough to extend to the main body of the gas phase. The bottom plate contained ports for liquid inlet and outlet. The top plate contained ports for the gas inlet and outlet, solution injection, and pH probe. The total volume of the reactor was 1.295 x 10^{-3} m^3.

The stirred cell contactor was equipped with Teflon-coated independently controlled agitators for gas and liquid phase mixing. Each agitator was driven by a Fisher StedFast Stirrer (Model SL 1200). The gas inlet was at the near center of the top plate, directly above the gas agitator blade, to ensure that the inlet gas was properly mixed. Gas and liquid agitation speeds were measured using a tachometer. The mass transfer coefficients (k_g, k_L^o) were a function of the agitation rates.

6.2 Gas source and flow path

Gas feed was prepared by quantitatively mixing 0.1% (1000 ppm) Cl_2 (in N_2) with nitrogen. The flow rates of all gas streams were controlled by Brooks mass flow controllers. The synthesized gas stream, typically at a flow rate of 1.2 L/min, was continuously fed to the reactor. After exiting the reactor, the gas stream was diluted with house air and continuously analyzed for chlorine. An empty 125-mL Erlenmeyer flask was connected after the reactor outlet to capture any water vapor or liquid. Since this flask stayed empty throughout an experiment, no liquid exited the reactor through the gas outlet. When the chlorine concentration to the reactor was less than 30 ppm, approximately 3 L/min of dilution air was used. When the chlorine concentration was greater, 36 L/min of dilution air was used. The chlorine analyzer output was connected to a strip chart recorder. The flux of chlorine (rate of chlorine absorption) was calculated from the gas phase material balance. An analyzer with an electrochemical sensor (NOVA Model 540P) was initially used. Later experiments were done using ion mobility spectrometry (Molecular Analytics AirSentry 10-Cl2).

6.3 Analyzer calibration

The chlorine analyzer was calibrated at the beginning and end of each experimental series to check for analyzer drift. There was essentially no drift for the IMS analyzer. During calibration, the gas flow rate was identical to that in an experiment. Other than bypassing the reactor, the gas flow path during calibration was the same as during an experimental run. To calibrate the analyzer zero, nitrogen (without chlorine) was supplied and diluted with house air. To calibrate the span, the gas flow rates were adjusted to give different chlorine concentrations spanning the range of interest. For the later experiments (those analyzed by IMS), both dry gas and wet gas calibrations were done to ensure that moisture did not affect the analyzer reading. Wet gas calibrations were done by having the nitrogen (not the chlorine) go through the stirred cell reactor filled with aqueous solution. For chlorine concentrations less than 30 ppm, there was a slight difference in wet and dry gas calibrations, probably resulting from the increased humidity of the gas. Therefore, wet calibrations were always used whenever experiments were done in which the chlorine concentration would be less than 30 ppm.

6.4 Electrochemical analyzer

The analyzer contains an electrochemical sensor with a platinum measuring electrode and silver reference electrode. The electrolyte used is a 3% lithium chloride solution. The electrolyte continuously weeps over the active surface of the sensor. When the chlorine contacts the electrochemical sensor, it reacts to form silver chloride (AgCl) which releases two electrons. The current produced is proportional to the chlorine concentration. Nitrogen dioxide (NO_2) and sulfur dioxide (SO_2) interfere with the electrochemical sensor analysis.

6.5 IMS analyzer

The analyzer is based on ion mobility spectrometry (IMS), similar in principle to time-of-flight mass spectrometry. The sample is passed over a semi-permeable membrane through which the chlorine diffuses. Purified dry instrument air (supplied externally) sweeps the chlorine from the interior of the membrane and into an ionization region supplied with a β^- source (Ni^{63}). The ionized molecules then drift through a cell under the influence of an electric field. An electronic shutter grid allows periodic introduction of the ions into a drift tube where they separate based on charge, mass, and shape. Smaller ions move faster than larger ions through the drift tube and arrive at the detector. The current created at the detector is amplified, measured as a function of time, and a spectrum is generated. A microprocessor evaluates the spectrum for the chlorine and determines the concentration based on peak height.

The IMS analyzer is linear throughout the entire range and can detect chlorine at very low concentrations. The IMS analyzer also has much better repeatability than the electrochemical sensor analyzer. The following do not interfere with the chlorine analysis: CO_2, Hg, SO_2, NO, hydrocarbons, and chlorinated hydrocarbons. However, NO_2 and HCl do interfere with the IMS analysis due to peak overlap at high concentrations.

6.6 Absolute chlorine analysis through wet chemical methods

The absolute gas phase chlorine concentration was measured using a wet chemical method. During these analyses, the gas flowed from the cylinder through the same tubing it would normally flow through in an experiment. The absolute chlorine concentration was measured (instead of relying on that of the gas supplier) since the analysis would yield the actual chlorine concentration that the reactor sees by accounting for chlorine loss between the cylinder and reactor (such as adsorption in tubing). At the beginning and end of each experiment, the tubing was flushed with nitrogen. Since no chlorine was detected by the analyzer under these conditions, chlorine desorption from tubing did not occur.

For many of the data analyses, absolute values for the chlorine concentration do not matter as much since relative chlorine concentrations are the important parameter. Usually in the data interpretation, the flux is normalized by the chlorine concentration, which is why only relative values are important. Also, in order to calculate the fraction gas film resistance (which is used to analyze some of the data), only relative concentrations are needed. The absolute value of the chlorine concentration does matter if only chlorine flux is looked at alone without normalizing it.

Initially, the absolute chlorine concentration was analyzed by sparging chlorine into a potassium iodide solution buffered at pH 5. Chlorine reacts with iodide to form iodine, which is then titrated with sodium thiosulfate to give the chlorine concentration. This method was the basis used for the initial analysis. Later on, the absolute chlorine was analyzed by sparging chlorine into sodium sulfite solution at pH 12.5 and then analyzing the chloride concentration using ion chromatography. For each mole of chlorine

absorbed, two moles of chloride are formed. This method resulted in a chlorine concentration 1.4 times what was seen in the early data (using the iodide method). The sulfite method gave more reproducible results and recovered more of the chlorine than the previously used potassium iodide method. For both of these methods, the zero was calibrated by supplying only nitrogen (without chlorine) through the tubing. Also, different chlorine concentrations were used in the experiment in order to verify the wet chemical method. Using the sulfite analysis, the cylinder chlorine concentration (after passing from the cylinder through the tubing) was 840 ppm, while Air Products stated that the cylinder concentration was 1000 ppm. Air Products also stated that the cylinder chlorine concentration may decrease over time, but they were not sure what the time span would be. A basis of 840 ppm was assumed for most of the data. For the earlier data, a basis of 600 ppm was used since the iodide method was employed. Multiplying the old data by 1.4 (840/600) will convert the magnitudes of the earlier data to that of the new data.

6.7 Reactor solution and analysis

The reactor contained the aqueous S(IV) solution, ranging from 0 to 10 mM, used in absorbing chlorine. The reactor fluid volume in a typical experiment was 1.06×10^{-3} m^3. Distilled water was first added to the reactor. For experiments at pH $\approx$ 4, the reactor solution was buffered by injecting a stock solution of equimolar succinic acid/sodium succinate. The buffer concentration in the reactor ranged from 5 to 50 mM total succinate. The S(IV) solution was obtained by injecting a stock solution containing equimolar sodium sulfite and sodium bisulfite. For experiments at pH > 7, stock solutions of only sodium sulfite were used.

Liquid samples (2 to 25 mL, depending on S(IV) concentration) were periodically taken from the bulk of the reactor and analyzed for S(IV) concentration by iodometric titration (Kolthoff and Belcher, 1957), and some samples were analyzed for chloride using ion chromatography. Withdrawing samples did not affect the reaction since each withdrawal was followed by subsequent injection of fluid.

The pH of the bulk reactor solution was continuously monitored and recorded using a strip chart recorder. The pH probe was calibrated by placing it into a standard pH 4 and pH 7 buffer solution. After calibration, the pH probe was inserted into the reactor fluid for continuous pH monitoring of the bulk reactor fluid. The pH was measured to verify that the experiments were being conducted at the desired pH. The concentration of each S(IV) species (bisulfite and sulfite) can be calculated by knowing the pH and total S(IV) concentration. In the buffered S(IV) experiments, essentially all of the S(IV) was present as bisulfite since the pH was much lower than the pK_a of the sulfite/bisulfite reaction.

6.8 Iodometric titration for S(IV)

After the S(IV) sample was withdrawn from the reactor, it was directly injected into excess iodine solution to avoid air oxidation to sulfate. The S(IV) reduced the iodine to iodide. The excess iodine was titrated with sodium thiosulfate. When the yellow color of the iodide started to fade (as the iodine was reduced to iodide by the thiosulfate), a couple

drops of starch indicator were added to enhance the endpoint detection. The endpoint was reached when the blue solution turned clear.

The S(IV) concentration was determined from the difference between the amount of thiosulfate used to titrate the excess iodine and the amount needed if no S(IV) were added to the iodine. The difference indicates how much of the iodine reacted with S(IV).

The S(IV) analysis procedure was modified as experiments were done. The S(IV) concentrations were more precise in the data taken after that in Table 8-5 because of procedural modifications such as checking blanks and verifying standard solutions daily and withdrawing larger samples from the reactor. However, at very low S(IV), the difference to determine the amount of iodine which reacted with S(IV) was very low. At times, it was close to the errors in measurements (buret readings). Thus, the expected precision at S(IV) concentrations below 0.09 mM is ± 0.04 mM. For example, when the S(IV) concentration is reported as 0.08 mM, the actual concentration could range from 0.04 to 0.12 mM.

7. Characterizing Stirred Cell Contactor

The overall resistance to mass transfer is equal to the sum of the resistances in the gas and liquid phases:

$$\frac{1}{K_{OG}} = \frac{1}{k_g} + \frac{H}{Ek_L^o} \tag{7-1}$$

If a reaction is very fast (high E) and/or if the gas is extremely soluble in the liquid (high H), the last term vanishes, and the overall gas mass transfer coefficient is equivalent to the individual gas film mass transfer coefficient. Therefore, k_g can be easily determined by absorbing a gas into a liquid which has a rapid reaction rate. On the other hand, if the gas has a low solubility (low H) and does not react quickly in the liquid, the resistance in the liquid film dominates the overall mass transfer resistance. Thus, to determine the liquid film mass transfer coefficient, gas should be desorbed from a liquid in which the gas is not very soluble. These criteria led to the experiments which were conducted to characterize the stirred cell contactor. Mass transfer coefficients are independent of chlorine concentration.

7.1 Gas film mass transfer coefficient

The gas phase mass transfer coefficient was obtained by measuring chlorine absorption in 0.28 M sodium hydroxide. Since the chlorine/hydroxide reaction is very fast, there is negligible resistance in the liquid phase; thus, K_{OG} is equivalent to k_g. Under complete gas film control, there is essentially no chlorine at the interface.

$$k_g = \frac{N_{Cl_2}}{P_{Cl_2,o}} \tag{7-2}$$

Figure 7-1 depicts the data and correlations for obtaining k_g, and Table 7-1 lists the correlation parameters. Detailed experimental data are in Appendix A. Data were taken under three analyzer conditions. Series A-1 displays the correlation obtained using the IMS analyzer. This correlation was used for all data obtained using the IMS analyzer. Series A-2 displays the correlation obtained from using the improved calibration (Figure 8-2) of the electrochemical analyzer. This correlation was used to analyze the chlorine absorption data in Table 8-5. Series A-3 shows the correlation obtained from using the electrochemical analyzer after experimental modifications were made to reduce scatter. This correlation was used for the data in Tables 8-6 and 8-7. Tables A-1 through A-3 tabulate the data used to obtain the above correlations.

The k_g correlations were compared with each other and with other correlations developed by previous researchers who used a similar apparatus. Zhao, who used the exact same apparatus, developed a k_g correlation for mercury by absorbing mercury into aqueous permanganate. Her correlation was: $k_g(\text{mol/s-atm-m}^2) = 0.0344(n_g)^{0.38}$ (Zhao and Rochelle, 1996). Dutchuk, who used a similar apparatus (but not identical), developed a k_g correlation for sulfur dioxide by absorbing SO_2 into sodium hydroxide. His correlation

was: $k_g(mol/s\text{-}atm\text{-}m^2) = 0.0552(n_g)^{0.385}$ (Dutchuk, 1999). Figure 7-1 and Table 7-1 display all the correlations.

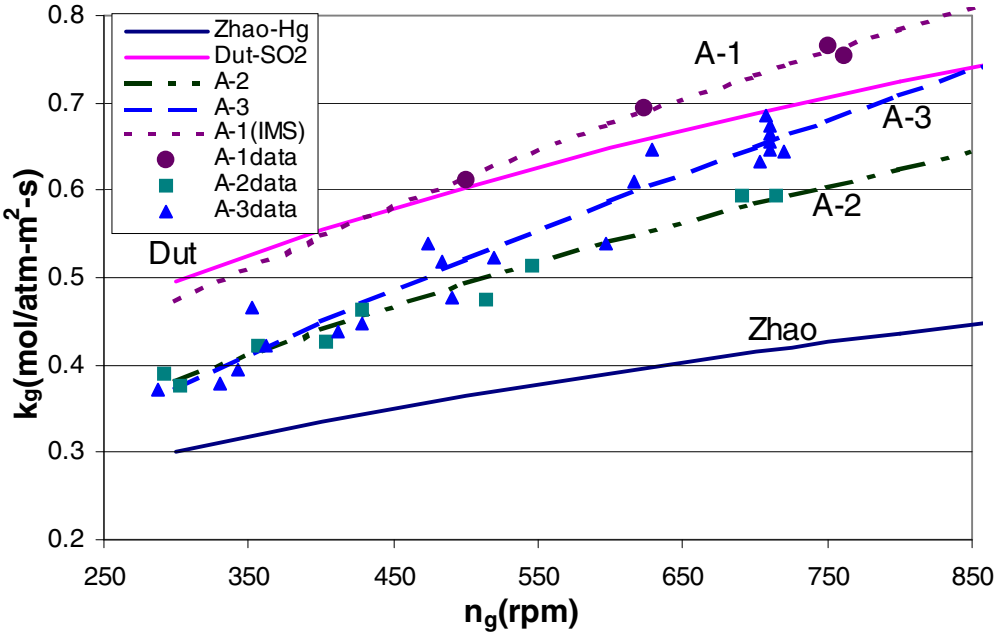

Figure 7-1. Data and correlations for gas film mass transfer coefficient

Table 7-1. Parameters for gas film mass transfer correlations

	$k_g=an_g^b$	
Series	a	b
A-1	0.0252	0.5142
A-2	0.0218	0.5018
A-3	0.0089	0.655
Zhao-Hg	0.0344	0.38
Dutchuk-SO_2	0.0552	0.385

Typical gas phase agitation rates (n_g) for the chlorine absorption in S(IV) experiments ranged from 650 to 750 rpm.

7.2 Liquid film mass transfer coefficient

The liquid phase mass transfer coefficient was obtained by measuring chlorine desorption from hypochlorous acid (HOCl) solution in 0.1 M HCl at ambient temperature. In a typical experiment, sodium hypochlorite (NaOCl) was injected into 1.06 L of 0.1 M HCl. At a flow rate of 1.2 L/min, nitrogen gas flowed over the solution, desorbing chlorine. The chlorine formation resulted from the following reaction:

$$Cl_2 + H_2O \leftrightarrow HOCl + Cl^- + H^+ \qquad (7\text{-}3)$$

At low pH and high chloride, the formation of chlorine is favored.

The liquid film mass transfer coefficient can be determined by correlating the chlorine concentration as a function of time. Liquid phase mass balance gives:

$$V\frac{dC_{Cl_2}}{dt} = -k^{o}_{L,Cl_2}A(C_{Cl_{2,b}} - C_{Cl_{2,i}}) \tag{7-4}$$

With excess gas, the chlorine at the interface is negligible compared to the chlorine in the bulk liquid. Thus, the mass balance in Equation 7-4 can be simplified and rearranged to yield:

$$\frac{dC_{Cl_2}}{C_{Cl_{2,b}}} = -\frac{k^{o}_{L,Cl_2}A}{V}dt \tag{7-5}$$

Integrating the above differential equation results in:

$$C_{Cl_{2,b}} = C_{Cl_{2,init}}\exp\left(-\frac{k^{o}_{L,Cl_2}A}{V}t\right) \tag{7-6}$$

Since the gas phase flux equals the liquid phase flux:

$$\frac{G\left(P_{Cl_{2,out}} - P_{Cl_{2,in}}\right)}{RT} = k^{o}_{L,Cl_2}A\left(C_{Cl_{2,b}} - C_{Cl_{2,i}}\right) \tag{7-7}$$

Since there is no chlorine in the entering gas, $P_{Cl_{2,in}} = 0$, and since the interfacial chlorine concentration is much less than the bulk chlorine concentration:

$$P_{Cl_{2,out}} = \frac{RT}{G}k^{o}_{L,Cl_2}AC_{Cl_{2,b}} \tag{7-8}$$

Combining the gas balance with the liquid balance and taking natural logarithms results in:

$$\ln P_{Cl_{2,out}} = \ln\left(\frac{RTC_{Cl_{2,init}}k^{o}_{L,Cl_2}A}{G}\right) - \frac{k^{o}_{L,Cl_2}A}{V}t \tag{7-9}$$

Therefore, from a plot of $\ln P_{Cl_{2,out}}$ vs time, the liquid film mass transfer coefficient can be extracted from the slope. Figure 7-2 shows the data and correlations for the liquid film mass transfer coefficient. All data were taken with the IMS analyzer. Detailed experimental data are in Appendix B.

The k^{o}_{L,Cl_2} correlation was compared with Zhao's correlation. Zhao performed mercury desorption experiments in the stirred cell contactor and found the correlation for mercury

to be $k^{o}_{L,Hg}$ (m/s) = 2.42 x $10^{-7}(n_L)^{0.73}$ (Zhao, 1997). The correlation for mercury was converted to a correlation for chlorine by correcting for diffusivities:

$$k^{o}_{L,Cl_2} = k^{o}_{L,Hg}\sqrt{\frac{D_{Cl_2}}{D_{Hg}}} \qquad (7\text{-}10)$$

Applying this correction resulted in: k^{o}_{L,Cl_2} (m/s) = 2.7 x $10^{-7}(n_L)^{0.73}$. Figure 7-2 shows how the correlation from this work compares with Zhao's corrected correlation. The solid line represents Zhao's correlation.

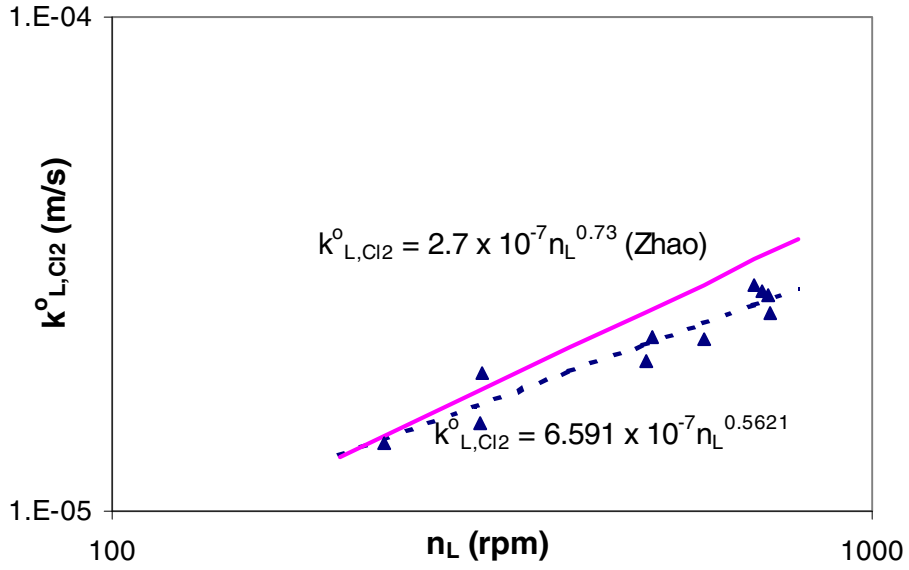

Figure 7-2. Data and correlations for physical liquid film mass transfer coefficient

In order to calculate the S(IV) at the interface, the liquid film transfer coefficient for S(IV) was needed. Thus, the above correlation, k^{o}_{L,Cl_2} (m/s) = 6.591 x $10^{-7}(n_L)^{0.56}$, was corrected for S(IV) by correcting for the diffusivities, which resulted in $k^{o}_{L,S(IV)}$ (m/s) = 6.248 x $10^{-7}(n_L)^{0.56}$. Table 7-2 lists the values for the diffusivities of mercury, chlorine, and S(IV) through water.

Table 7-2. Diffusivity for species used to correct k^{o}_{L} correlations

D_{Hg} (m^2/s)[a]	1.2 x 10^{-9}
D_{Cl_2} (m^2/s)[b]	1.48 x 10^{-9}
$D_{S(IV)}$ (m^2/s)[c]	1.33 x 10^{-9}

[a] obtained from Zhao (1997)
[b] obtained from Spalding (1962)
[c] obtained from Chang (1979)

8. Tabulated Results

8.1 Preliminary results with the electrochemical analyzer

Tables 8-1 and 8-2 display initial chlorine absorption data. Gaseous chlorine was analyzed using the electrochemical sensor analyzer for these data except for data in Table 8-1 Series A, which were analyzed using the wet chemical iodide method (since the continuous chlorine analyzer had not been purchased yet). A linear calibration was used for the electrochemical analyzer. For the absolute values of the chlorine concentration, the iodide wet chemical method was used. As noted earlier, the magnitude of these data are 1.4 times less than later data calculated using the sulfite method.

Table 8-1. Initial chlorine absorption results, electrochemical sensor analyzer

Series	pH	[S(IV)](mM)	n_g(rpm)	n_L(rpm)	$Cl_{2,in}$(ppm)	$Cl_{2,out}$(ppm)	N_{Cl2}(kmol/m^2-s)
A	8	5.5	432	663	200	45	1.67E-08
	8.2	8.1	482	693	200	40	1.72E-08
	8.6	10	498	660	200	40	1.72E-08
	7.6	1.9	484	680	200	65	1.45E-08
B	water	0	533	609	204	170	3.65E-09
	6 - 7	2.51	533	609	204	63	1.51E-08
	6 - 7	2.48	533	609	204	50.7	1.65E-08
C	water	0	555	620	204	161	4.58E-09
	4.5	0	555	620	204	175	3.12E-09
	4.5	2.9	555	620	204	93.3	1.19E-08
D	4 - 4.5	0	521	640	204	172	3.49E-09
	4 - 4.5	3.44	521	640	204	79.6	1.34E-08
	4 - 4.5	1.3	554	640	204	113	9.78E-09
	4 - 4.5	1.3	554	640	204	136	7.30E-09
	4 - 4.5	0.68	554	640	204	142	6.66E-09
	4 - 4.5	2.12	554	640	204	61.9	1.53E-08

All the data in Table 8-2 were obtained with a succinic acid/succinate buffer. These data were also taken with the electrochemical sensor analyzer using a linear calibration. However, it was later discovered that the calibration was not entirely linear, and a linear calibration overpredicted the concentration.

Table 8-2. Chlorine absorption in pH 4-4.5 S(IV) with incorrect analyzer calibration of electrochemical sensor analyzer

Series	[S(IV)](mM)	n_g (rpm)	n_L (rpm)	$Cl_{2,in}$(ppm)	$Cl_{2,out}$(ppm)	N_{Cl2}(kmol/m^2-s)
A	4.2	619	740	200	97	1.11E-08
	3.58	619	740	200	105	1.02E-08
	2.19	619	740	200	94	1.14E-08
B	0	592	578	200	183	1.83E-09
	4.32	604	567	200	106	1.01E-08
	3.32	604	567	200	156	4.73E-09
	1.16	604	567	200	161	4.19E-09
	1.4	605	574	200	113	9.35E-09
	1.19	603	575	155	83	7.75E-09
	1.16	603	575	155	93	6.60E-09
C	0	535	560	200	166	3.71E-09
	3.84	535	560	200	96	1.12E-08
	3	590	569	200	103	1.04E-08
	2.68	573	568	200	111	9.56E-09
	2.25	573	568	200	128	7.73E-09
	0.67	579	573	200	157	4.62E-09
	0.60	579	573	168	148	2.18E-09
	5.27	579	573	168	79	9.54E-09

8.2 Results obtained using multi-point calibration of the electrochemical analyzer

Since the analyzer output was not linear over the entire range, a multi-point calibration was performed. Also due to problems with analyzer drift, calibration was checked several times within a series of experiments. Figure 8-1 displays a typical chlorine analyzer multi-point calibration.

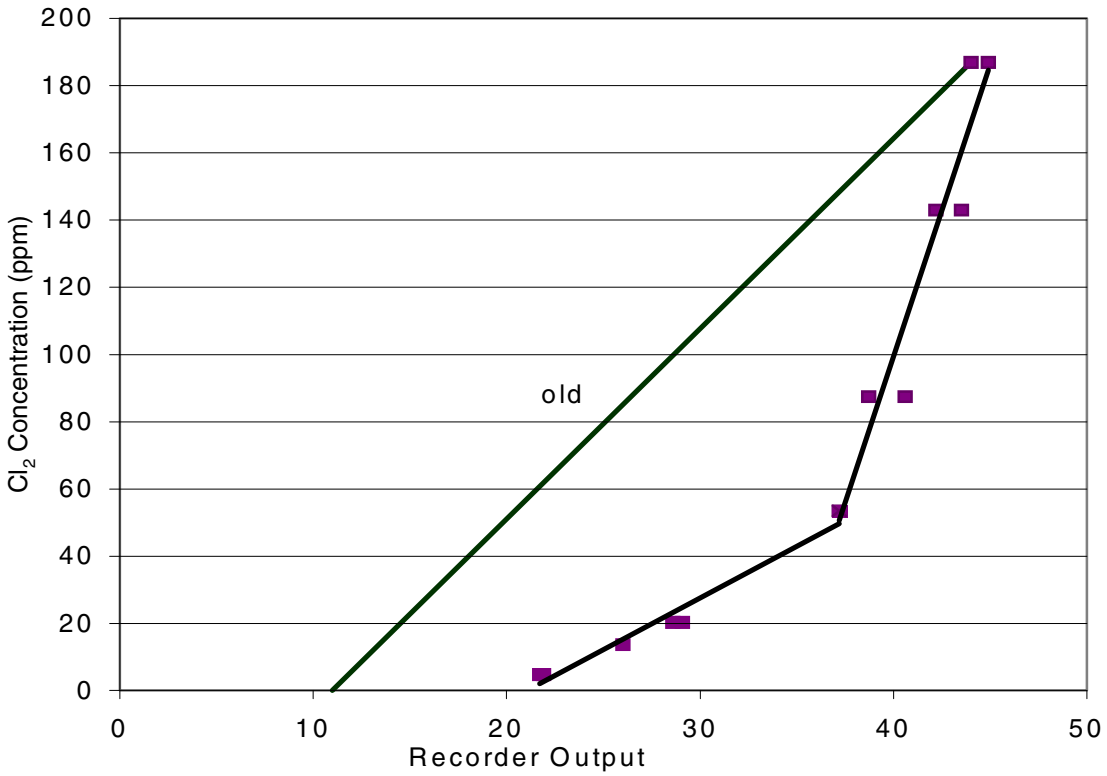

Figure 8-1. Electrochemical chlorine analyzer multi-point calibration

The "old" line represents the linear calibration previously used for much of the data. Using the linear calibration greatly overpredicts the chlorine concentration. The two-line (multi-point) calibration demonstrates the nonlinearity and reproducibility problem of the analyzer. Using this two-line calibration, errors in chlorine concentration can be as much as ± 20 ppm. Table 8-3 displays data using the two-line calibration shown in Figure 8-1.

Table 8-3. Chlorine absorption in buffered S(IV) using multi-point calibration

buffer(mM)	[S(IV)](mM)	$Cl_{2,in}$(ppm)	$Cl_{2,out}$(ppm)	N_{Cl2}(kmol/m^2-s)	K_{OG}/kg(%)	[Cl^-] (mM)
10	0	179	127	5.75E-09	11.4	0.19
10	0	170	129	4.53E-09	8.9	0.21
10	0	170	129	4.53E-09	8.9	0.30
50	0.31	184	118	7.24E-09	15.3	2.0
10	0.36	179	90	9.82E-09	27.5	0.87
50	0.46	183	156	2.96E-09	4.8	2.49
50	0.50	186	153	3.65E-09	5.9	5.4
10	0.50	179	104	8.31E-09	20.2	0.71
50	0.77	183	90	1.03E-08	28.7	2.24
50	0.88	183	80	1.14E-08	35.8	1.74
10	0.92	151	65	9.51E-09	36.6	1.47
50	0.94	184	113	7.82E-09	17.3	1.0
10	1.12	179	67	1.24E-08	46.3	0.33
10	1.85	151	21	1.44E-08	172.5	0.41
50	2.57	186	53	1.48E-08	70.4	2.5

8.3 Results obtained using improved calibration of electrochemical analyzer

After the above data were taken, the nonlinearity and reproducibility problem shown in Figure 8-1 was solved. The problem occurred because the electrochemical cell was not completely full of electrolyte. Table 8-4 and Figure 8-2 display the new improved calibration after this problem was remedied.

Table 8-4. Electrochemical chlorine analyzer calibration after fixing electrolyte level

Recorder output	ppm Cl_2
88.7	187
74.3	143
55.5	87.5
74.7	143
88.8	187
74.6	143
54.9	87.5
41.4	53.5
33.4	31.3
28.3	20.4
24.8	13.7
17.7	4.79
25.0	13.7
28.6	20.4
17.5	4.79
28.2	20.4
33.5	31.3
43.8	53.5

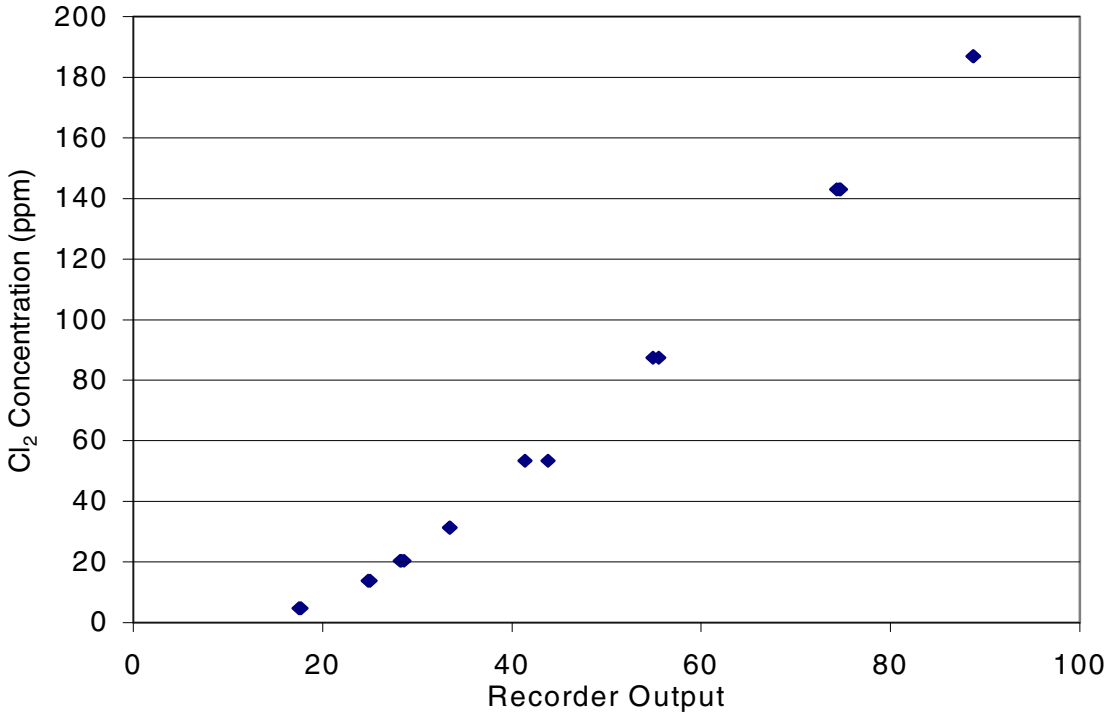

Figure 8-2. Improved calibration of electrochemical chlorine analyzer

As seen from Table 8-4 and Figure 8-2, fixing the electrolyte problem greatly improved reproducibility. Using this improved calibration for the electrochemical sensor analyzer, chlorine concentrations greater than 100 ppm usually had a reproducibility of ± 8 ppm while concentrations less than 100 ppm had a reproducibility of ± 2 ppm. Table 8-5 displays data which were taken using this type of calibration.

Table 8-5. Chlorine absorption in S(IV) solutions using improved calibration of the electrochemical analyzer, 1.29 L/min gas, 50 mM buffer, k_g = 0.6 mol/s-atm-m^2

Series	[S(IV)](mM)	$Cl_{2,in}$(ppm)	$Cl_{2,out}$(ppm)	N_{Cl2}(kmol/m^2-s)	K_{OG}/kg(%)	[Cl^-](mM)
A	0*	197	136	6.07E-09	8.2	0.18
	1.76*	197	44	1.54E-08	64.7	1.15
	1.3*	197	74	1.23E-08	30.1	1.92
	1.31	197	80	1.17E-08	26.7	1.75
	1.14	197	141	5.60E-09	7.2	3.18
	0.94	197	145	5.20E-09	6.5	2.87
B	0	197	120	7.72E-09	11.8	0.09
C	0	197	129	6.82E-09	9.4	0.09
	1.19	197	101	9.60E-09	16.9	0.87
	0.81	197	132	6.55E-09	8.9	1.22
	0.68	197	135	6.20E-09	8.2	1.51
	2.04	197	59	1.39E-08	41.8	1.97
	1.05	197	93	1.04E-08	19.9	2.68
	0.90	197	116	8.08E-09	12.3	3.04

* Experiments in 10 mM succinate buffer instead of 50 mM succinate buffer

The experimental scatter in the above data was resolved by modifying the experimental analysis. The precision in the S(IV) concentration measurements was greatly enhanced by increasing sample size and verifying standard solutions daily. Also, scatter was reduced by lowering the pressure in the reactor, which minimized leaks. The absolute chlorine concentration was now obtained using the sulfite method since it gave better results than the previously used iodide method. So, the magnitudes are all 1.4 times higher than what was previously reported. Tables 8-6 and 8-7 show data obtained after these modifications were made. The data in Table 8-6 are for chlorine inlet concentrations greater than 100 ppm, while the data in Table 8-7 are for chlorine inlet concentrations of 21 ppm.

Table 8-6. Chlorine absorption in pH 4.3 - 4.5 S(IV), measured with electrochemical analyzer, 1.2 L/min gas, 50 mM succinate buffer, and k_g = 0.60 – 0.66 mol/s-atm-m^2

Series	[S(IV)](mM)	$Cl_{2,in}$(ppm)	$Cl_{2,out}$(ppm)	N_{Cl2}(kmol/m^2-s)	K_{OG}/kg(%)	[Cl^-] (mM)
A	0	276	185	9.13E-09	8.2	0.36
	1.19	276	118	1.59E-08	22.5	0.5
	0.88	276	177	9.94E-09	9.4	0.76
	0.43	276	222	5.37E-09	4.0	1.1
	1.21	276	132	1.45E-08	18.3	1.65
	0.87	276	162	1.15E-08	11.8	6.56
	0.78	276	184	9.18E-09	8.2	19.7
B	0	276	174	1.02E-08	9.5	0.12
	1.45	276	70	2.06E-08	47.7	1.13
	0.95	276	141	1.35E-08	15.4	1.32
	0.84	129	43	8.86E-09	33.5	1.3
	0.62	129	50.4	8.07E-09	25.9	2.88
	0.58	276	181	9.55E-09	8.5	1.49
C	0	276	179	9.69E-09	8.3	0.17
	1.37	276	51.5	2.25E-08	37.0	0.86
	1.25	276	80.6	1.96E-08	29.5	1.61
	0.82	276	94.1	1.82E-08	53.7	1.9
	0.69	129	29.1	1.03E-08	8.8	2.31

Table 8-7. Chlorine absorption measured with electrochemical analyzer in pH 4.5 S(IV), $Cl_{2,in}$ = 21 ppm, 1.19 L/min gas, 50 mM succinate buffer

Series	$[S(IV)]_{bulk}$(mM)	$Cl_{2,in}$(ppm)	$Cl_{2,out}$(ppm)	N_{Cl2}(kmol/m^2-s)
A	1.16	21	2.9	1.85E-09
	1.14	21	2.9	1.85E-09
B	0.23	21	9.5	1.17E-09
	0.20	21	12.2	8.98E-10
	0.13	21	14.0	7.17E-10
C	0.20	21	9.9	1.13E-09
D	0.31	21	6.4	1.49E-09
	0.27	21	7.9	1.34E-09

8.4 Results obtained using the IMS chlorine analyzer

The above data were the last set obtained using the electrochemical analyzer. The next set of experiments were done using the IMS analyzer with the following conditions in mind: 1) experiments at low chlorine and S(IV) concentrations to extract kinetics, 2) experiments with oxygen in the inlet gas, 3) experiments at high S(IV) concentrations to quantify S(IV) oxidation rates and see if chlorine catalyzes S(IV) oxidation. Table 8-8 displays the first set of data using the IMS analyzer, including data with oxygen. Table 8-9 lists data for oxygen absorption in S(IV). Table 8-10 lists the final set of data in 50 mM succinate buffer.

Table 8-8. Chlorine and oxygen absorption measured with IMS analyzer in pH 4.5 S(IV), 50 mM succinate buffer, and 1.15 L/min gas

Series	$[S(IV)]_{bulk}$(mM)	$Cl_{2,in}$(ppm)	$Cl_{2,out}$(ppm)	N_{Cl2}(kmol/m^2-s)	O_2 (%)
A	0*	276	235	4.09E-09	0
	0*	276	242	3.37E-09	0
	0	276	150	1.26E-08	0
	1.15	276	94.6	1.82E-08	0
	0.78	129	21.6	1.10E-08	0
	0.634	21	2.5	1.93E-09	0
	4	276	33.8	2.43E-08	0
	4	129	10.8	1.21E-08	0
	4	129	13.2	1.19E-08	0
	4	21	0.33	2.14E-09	0
B	0*	276	225	5.10E-09	0
	0*	276	236	3.99E-09	0
	0	276	151	1.25E-08	0
	3.85	276	34.5	2.42E-08	0
	2.44	276	39.3	2.37E-08	0
	1.86	276	39.7	2.37E-08	0
C	0	276	149	1.27E-08	0
	5.04	276	37.5	2.39E-08	0
	3	276	38.5	2.38E-08	0
	1.74	276	43.7	2.33E-08	0
D	0*	21	15.6	5.46E-10	0
	0*	21	17	4.05E-10	0
	0	21	8.3	1.28E-09	0
	5	21.2	1.3	2.01E-09	0
E	0	264	134	1.26E-08	14.5
	4.43	264	32.7	2.24E-08	14.5
	3.83	264	28	2.29E-08	14.5
	3.22	264	31.7	2.25E-08	14.5
	2.02	264	39	2.18E-08	14.5
	1.37	264	41.9	2.15E-08	14.5
	0.664	264	116	1.44E-08	14.5
	0.35	264	159	1.02E-08	14.5
F	0	21	8.1	1.31E-09	0

(Continued)

Table 8-8. Continued

Series	$[S(IV)]_{bulk}$(mM)	$Cl_{2,in}$(ppm)	$Cl_{2,out}$(ppm)	N_{Cl2}(kmol/m^2-s)	O_2 (%)
G	0	21.2	8	1.33E-09	0
	0.26	21.2	3.8	1.76E-09	0
	0.176	21.2	4.7	1.66E-09	0
	1.08	21.2	2.2	1.92E-09	0
	1.05	21.2	2.04	1.93E-09	0
	1.02	21.2	2.15	1.92E-09	0
	3.74	21.2	0.9	2.05E-09	0
	3.44	21.2	1.2	2.02E-09	0
	3.43	21.2	1	2.04E-09	0
	3.59	21.2	1	2.04E-09	0
H	0	21.2	7.9	1.34E-09	20.5
	0.519	21.2	2.99	1.84E-09	20.5
	0.336	21.2	3.6	1.78E-09	20.5
	0.18	21.2	4.3	1.70E-09	20.5
	1.56	21.2	1.5	1.99E-09	20.5
	1.18	21.2	1.9	1.95E-09	20.5
	0.642	21.2	2.5	1.89E-09	20.5
	4.74	21.2	0.8	2.06E-09	20.5
	4.23	21.2	0.94	2.04E-09	20.5
	3.88	21.2	1	2.04E-09	20.5

* not buffered; absorption in pure water

Table 8-9. S(IV) depletion resulting from oxygen absorption in pH 4.5 S(IV) at ambient temperature, 50 mM succinate buffer, and 1.15 L/min gas

Series	Δt(min)	$[S(IV)]_{bulk}$(mM)	O_2 (%)
A	0	6.06	14.5
	33	4.23	14.5
	37	4.07	14.5
	29	3.89	14.5
	57	3.86	14.5
	103	3.13	14.5
B	0	2.72	14.5
	53	2.36	14.5
C	0	4.88	20.5
	53	3.99	20.5
	42	3.64	20.5
	65	3.21	20.5
	60	2.66	20.5
	36	2.33	20.5
	37	2.18	20.5
	45	1.69	20.5
	57	1.27	20.5
	29	0.99	20.5

Table 8-10. Chlorine absorption in pH 4.5 S(IV), 50 mM succinate buffer, 1.15 L/min gas

Series	$[S(IV)]_{bulk}$(mM)	$Cl_{2,in}$(ppm)	$Cl_{2,out}$(ppm)	N_{Cl2}(kmol/m^2-s)
A	0	263.9	134.1	1.26E-08
	0	263.9	142.3	1.18E-08
	0.38	263.9	154.0	1.06E-08
	0.169	263.9	163.5	9.73E-09
	0.59	263.9	131.2	1.29E-08
	0.334	263.9	171.7	8.93E-09
	0.208	263.9	178.2	8.30E-09
	1.56	263.9	43.3	2.14E-08
	1.22	263.9	49.8	2.07E-08
	4.95	263.9	29.9	2.27E-08
	10	263.9	23.0	2.33E-08
B	0	21.2	4.35	1.70E-09
	0	21.2	4.89	1.65E-09
	0.182	21.2	3.67	1.77E-09
	0.075	21.2	7.75	1.36E-09
	0.276	21.2	3.84	1.75E-09
	0.178	21.2	4.62	1.67E-09
	1.38	21.2	2	1.94E-09
	1.32	21.2	2	1.94E-09
	5.23	21.2	0.7	2.07E-09
	10	21.2	0.3	2.11E-09
C	0	263.9	132.5	1.27E-08
	0	263.9	142.2	1.18E-08
	0.27	263.9	153.5	1.07E-08
	0	263.9	163.5	9.73E-09
	0.61	263.9	125.0	1.35E-08
	0.437	263.9	160.0	1.01E-08
	1.25	263.9	46.5	2.11E-08
	0.74	263.9	94.7	1.64E-08
	4.7	263.9	32.0	2.25E-08
	10	263.9	24.9	2.32E-08
D	0	21.2	7.25	1.41E-09
	0.183	21.2	4.24	1.71E-09
	0.098	21.2	6.68	1.46E-09
	0.26	21.2	3.83	1.75E-09
	0.128	21.2	5.69	1.56E-09
	1.43	21.2	2.2	1.92E-09
	1.39	21.2	2.2	1.92E-09
	5.45	21.2	0.6	2.08E-09

8.5 Chlorine absorption as a function of succinate buffer concentration

Experiments were done to study the effect of the succinate buffer on chlorine absorption. The reactor solution was buffered by injecting a stock solution of equimolar succinic acid/sodium succinate. The buffer concentration was varied from 0 to 150 mM total succinate. Table 8-11 lists data for chlorine absorption at various buffer concentrations in which no S(IV) is present.

Table 8-11. Chlorine absorption as a function of buffer concentration at ambient temperature in pH 4.5 with 1.15 L/min gas

Series	[buffer] (mM)	$Cl_{2,in}$ (ppm)	$Cl_{2,out}$(ppm)	N_{Cl2} (kmol/m^2-s)
A	0	21.2	13.83	7.40E-10
	0	21.2	14.85	6.37E-10
	10.3	21.2	11.82	9.44E-10
	48	21.2	8.61	1.27E-09
	48	21.2	9.00	1.23E-09
	66	21.2	8.04	1.33E-09
	102	21.2	7.33	1.40E-09
	102	21.2	7.15	1.42E-09
	137	21.2	6.71	1.46E-09
	154	21.2	6.76	1.46E-09
B	0	263.9	211.8	5.05E-09
	0	263.9	225.0	3.77E-09
	10.3	263.9	187.4	7.41E-09
	48	263.9	148.6	1.12E-08
	66	263.9	143.0	1.17E-08
	102	263.9	132.0	1.28E-08
	102	263.9	136.4	1.24E-08
	137	263.9	129.2	1.31E-08
	154	263.9	126.7	1.33E-08
C	0	263.9	175.4	8.57E-09
	0	263.9	203.1	5.89E-09
	10.3	263.9	182.2	7.92E-09
	48	263.9	148.1	1.12E-08
	66	263.9	139.6	1.20E-08
	102	263.9	126.8	1.33E-08
	137	263.9	118.3	1.41E-08
	154	263.9	116.5	1.43E-08

8.6 Chlorine absorption in 5 mM succinate buffer

Since chlorine reacts with the buffer, future experiments were done in 5 mM buffer instead of 50 mM. These data are tabulated in Table 8-12. Lowering the buffer concentration lowered the chlorine flux in the buffer, resulting in a wider range of fluxes between the limitations of the chlorine/buffer and of gas film control.

Table 8-12. Chlorine absorption in pH 4.5 S(IV), 5 mM buffer, 1.18 L/min gas

Series	$[S(IV)]_{bulk}$(mM)	$Cl_{2,in}$(ppm)	$Cl_{2,out}$(ppm)	N_{Cl2}(kmol/m^2-s)
E	0	21.2	12.9	8.39E-10
	0.213	21.2	4.33	1.70E-09
	0.155	21.2	5.51	1.58E-09
	0.103	21.2	8.88	1.24E-09
	0.089	21.2	13.6	7.63E-10
	1.48	21.2	2.23	1.91E-09
F	0	21.2	13.0	8.21E-10
	0.117	21.2	7.49	1.38E-09
	0.076	21.2	11.6	9.66E-10
	0.064	21.2	13.51	7.73E-10
	0.06	21.2	15.1	6.17E-10
	0.15	21.2	6.09	1.52E-09
	0.12	21.2	9.26	1.20E-09

Table 8-13 tabulates the data in which agitation rates were varied. S(IV) concentrations were not measured for each point. The series of experiments began with chlorine absorption in 5 mM buffer. S(IV) was then injected and agitation rates were varied. At the end of the series, a sample was taken from the reactor and analyzed for S(IV). After the S(IV) was depleted, more was injected, and the agitation rates were varied.

Table 8-13. Chlorine absorption in S(IV) solutions with 5 mM buffer at various agitation rates

	[S(IV)](mM)	n_g (rpm)	n_L (rpm)	$Cl_{2,in}$(ppm)	$Cl_{2,out}$(ppm)	N_{Cl2}(kmol/m^2-s)
A	0	720	780	21.2	16.8	4.43E-10
A1	Inject S(IV)	720	780	21.2	4.69	1.67E-09
A1		720	780	21.2	5.91	1.54E-09
A1		720	472	21.2	9.87	1.14E-09
A1		720	472	21.2	10.5	1.08E-09
A1		720	472	21.2	10.8	1.05E-09
A1		720	898	21.2	6.82	1.45E-09
A1		720	1029	21.2	6.67	1.47E-09
A1		887	1036	21.2	7.16	1.42E-09
A1		1007	1039	21.2	7.43	1.39E-09
A1		1007	1039	21.2	7.74	1.36E-09
A1	0.11	752	757	21.2	12.3	8.97E-10
A2	Inject S(IV)	752	757	21.2	5.30	1.60E-09
A2		752	757	21.2	5.91	1.54E-09
A2		745	1053	21.2	5.23	1.61E-09
A2		382	1063	21.2	6.06	1.53E-09
A2		382	330	21.2	13.9	7.30E-10
A2		678	319	21.2	14.5	6.72E-10
A2		926	319	21.2	14.8	6.44E-10
A2		926	695	21.2	10.8	1.05E-09
A2		926	1051	21.2	7.74	1.36E-09

(Continued)

Table 8-13. Continued

	[S(IV)](mM)	n_g (rpm)	n_L (rpm)	$Cl_{2,in}$(ppm)	$Cl_{2,out}$(ppm)	N_{Cl2}(kmol/m^2-s)
A2		1051	757	21.2	12.0	9.25E-10
A2	0.078	1051	757	21.2	13.1	8.17E-10
B	0	730	708	21.2	14.8	6.44E-10
B1	Inject S(IV)	730	708	21.2	7.10	1.42E-09
B1		730	708	21.2	7.71	1.36E-09
B1		1151	713	21.2	8.94	1.24E-09
B1		344	713	21.2	9.86	1.14E-09
B1		344	713	21.2	10.5	1.08E-09
B1		332	402	21.2	14.8	6.44E-10
B1		332	402	21.2	15.1	6.16E-10
B1		330	1044	21.2	10.2	1.11E-09
B1		330	1044	21.2	10.5	1.08E-09
B1		974	1058	21.2	11.1	1.02E-09
B1		974	1058	21.2	11.4	9.88E-10
B1	0.070	749	762	21.2	14.6	6.60E-10
B1		748	408	21.2	15.8	5.42E-10
B1		749	1057	21.2	14.4	6.78E-10
B1		1140	1083	21.2	14.8	6.47E-10
B1		1153	722	21.2	16.1	5.08E-10
B1		734	717	21.2	16.3	4.92E-10
B2	0.028	734	717	21.2	16.6	4.61E-10
B3	Inject S(IV)	734	717	21.2	4.35	1.70E-09
B3		1054	715	21.2	4.10	1.72E-09
B3		1054	715	21.2	4.38	1.70E-09
B3		1069	341	21.2	8.48	1.28E-09
B3		478	336	21.2	9.24	1.20E-09
B3		467	990	21.2	5.14	1.62E-09
B3		1103	1004	21.2	4.20	1.72E-09
B3		720	1009	21.2	4.75	1.66E-09
B3	0.13	715	731	21.2	6.28	1.50E-09
B4	Inject S(IV)	715	731	21.2	2.91	1.85E-09
B4		711	408	21.2	3.06	1.83E-09
B4		369	403	21.2	4.10	1.72E-09
B4		366	938	21.2	3.98	1.74E-09
B4		1100	946	21.2	2.42	1.89E-09
B4		1113	383	21.2	2.54	1.88E-09
B4		1117	713	21.2	2.48	1.89E-09
B4	0.64	719	717	21.2	3.06	1.83E-09

9. Discussion of Results

9.1 Rate of reaction for chlorine with S(IV)

Figure 9-1 shows the data with the IMS analyzer (Tables 8-8, 8-10, and 8-12). Data at the two chlorine inlet concentrations of 265 ppm and 21 ppm are shown. The points at 0.01 mM S(IV) are actually in succinate buffer with no S(IV). The inverted triangles in Figure 9-1 represent points in which oxygen was added. At an inlet concentration of 265 ppm, the oxygen level was 14.5%, and at 21 ppm, the oxygen level was 20.5%. All the data are in 50 mM buffer except for the points represented by the squares with diagonal lines which are in 5 mM buffer.

The curves are calculated using the model for mass transfer with fast chemical reaction in the boundary layer. The model was similar to Equation 5-4, but included the buffer effect also:

$$N_{Cl_2} = \frac{P_{Cl_{2i}}}{H_{Cl_2}} \sqrt{D_{Cl_2}\left(k_{2,S(IV)}[S(IV)]_i + k_{2,buf}[buffer]\right)} \qquad (9\text{-}1)$$

The partial pressure of chlorine at the interface can be calculated from Equation 5-1, and the interfacial S(IV) concentration can be obtained from Equation 5-7. Substituting these into Equation 9-1 yields:

$$N_{Cl_2} = \frac{1}{H_{Cl_2}}\left(P_{Cl_2,b} - \frac{N_{Cl_2}}{k_g}\right)\sqrt{D_{Cl_2}\left(k_{2,S(IV)}\left([S(IV)]_b - \frac{N_{Cl_2}}{\Phi k^o_{L,S(IV)}}\right) + k_{2,buf}[buffer]\right)} \qquad (9\text{-}2)$$

The partial pressure of chlorine in the bulk (which is equivalent to the chlorine exiting the reactor) can be written in terms of the inlet chlorine concentration through a gas phase material balance. Thus, Equation 9-3 displays the model used to calculate the curves, and Table 9-1 lists the parameters that were supplied to the model.

$$N_{Cl_2} = \frac{1}{H_{Cl_2}}\left(P_{Cl_2,in} - \frac{N_{Cl_2}A}{G} - \frac{N_{Cl_2}}{k_g}\right)\sqrt{D_{Cl_2}\left(k_{2,S(IV)}\left([S(IV)]_b - \frac{N_{Cl_2}}{\Phi k^o_{L,S(IV)}}\right) + k_{2,buf}[buffer]\right)} \qquad (9\text{-}3)$$

Table 9-1. Values of parameters in global model

D_{Cl_2} (m^2/s)	1.5×10^{-9}
G (m^3/s)	0.0708 (1.18 L/min)
Φ	1
H_{Cl_2} (atm-m^3/kmol)	16.7
k_g (kmol/s-atm-m^2)	0.00075
$k^o_{L,S(IV)}$ (m/s)	2.45×10^{-5}
$k_{2,S(IV)}$ (L/mol-s)	2×10^{9}

The gas flow rate and mass transfer coefficients used in the model were representative of the experimental data. The stoichiometric coefficient, Φ, was chosen to be one because the overall stoichiometry of the reaction shows that one mole of chlorine reacts for every mole of S(IV). The buffer rate constant was obtained from the analysis of the chlorine absorption in succinate buffer experiments discussed in Section 9.3. The rate constant of the chlorine/S(IV) reaction ($k_{2,S(IV)}$) was chosen to best fit the data.

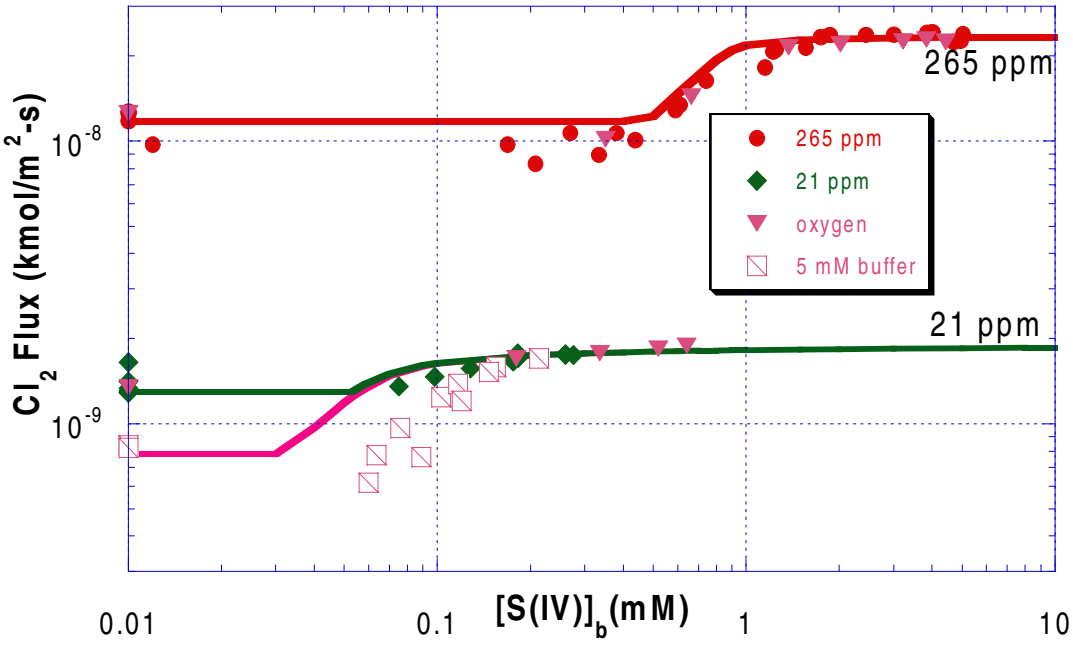

Figure 9-1. Chlorine absorption in buffered S(IV), $k_{2,S(IV)}$ = 2 x 10^9 L/mol-s

Figure 9-1 shows that at high S(IV), the chlorine flux does not depend on the S(IV) concentration since the limit of gas film resistance is approached. At lower chlorine concentrations, gas film control is achieved at lower S(IV) since it takes less S(IV) to react with the chlorine. Because of complete gas film control, the chlorine flux should not increase after 3 mM S(IV) with the 265 ppm chlorine inlet or after 0.6 mM S(IV) with 21 ppm inlet chlorine. However, the data at high S(IV) concentrations in Tables 8-8 and 8-10 show that additional chlorine removal is occurring at high S(IV). The additional chlorine removal is due to the increased levels of gaseous SO_2, which forms at high S(IV) concentrations, in the reactor:

$$SO_2(g) + H_2O \leftrightarrow H^+ + HSO_3^- \qquad (9\text{-}4)$$

At high S(IV) and low pH, the above reaction favors SO_2 production. The SO_2 reacts with the chlorine in the moist areas on the reactor surface. Therefore, Figure 9-1 plots all of the IMS analyzer data except for the values at S(IV) concentrations greater than 5 mM for the 265 ppm data and greater than 1 mM for the 21 ppm data. At pH 4.5, 5 mM S(IV) results in generation of about 70 ppm SO_2. Therefore, the existing stirred cell contactor cannot be used for experiments at high S(IV)/low pH since SO_2 would form inside the reactor.

Figure 9-1 shows that at low S(IV), the flux is limited (in some cases inhibited) by the buffer-enhanced chlorine hydrolysis reaction. In this region, the flux depends only on the buffer reaction rate. However, the data show that when very little S(IV) was injected, the chlorine flux was less than what it was initially in buffer alone. Thus, S(IV) inhibited chlorine absorption at very low S(IV) concentrations. At a chlorine concentration of 265 ppm and S(IV) concentration of 0.5 mM, the flux was equivalent to the flux in buffer alone. When the S(IV) concentration was lower, the flux was lower than what it was initially without S(IV). As the S(IV) increased, the chlorine flux increased until the gas film limit was reached. At the low inlet chlorine of 21 ppm, when the S(IV) concentration was 0.06 mM, the chlorine flux was the same as the flux in buffer alone. At lower concentrations, the flux is lower, and thus, the reaction seems to be inhibited by a little S(IV) but enhanced by greater amounts of S(IV).

Since Fogelman et al. (1989) have shown that HOCl reacts with sulfite, one possible mechanism for chlorine reaction with S(IV) is that the chlorine first hydrolyzes in water to form HOCl, and then the HOCl (not Cl_2 directly) reacts with S(IV). These overall reactions are shown below:

$$Cl_2 + H_2O \rightarrow HOCl + H^+ + Cl^- \quad (9\text{-}5)$$

$$HOCl + SO_3^{-2} \rightarrow SO_4^{-2} + H^+ + Cl^- \quad (9\text{-}6)$$

If this were the case, the rate of chlorine absorption in S(IV) would be equivalent to the rate of chlorine hydrolysis to form HOCl since chlorine hydrolysis is the rate limiting step. Then, the HOCl would react with S(IV). However, since the addition of S(IV) results in a greater chlorine removal rate than the chlorine hydrolysis rate, it must not depend on HOCl formation. Thus, chlorine itself reacts with S(IV) directly, and it is not necessary for HOCl to form before chlorine reaction with S(IV) occurs.

In the intermediate region of Figure 9-1, the flux is limited by S(IV) diffusion to the interface [depicted by flux increasing linearly with S(IV)] and/or kinetics (depicted by curvature). Looking at the 265 ppm data, for S(IV) between 0.5 and 0.8 mM, the flux increases linearly with S(IV), which is consistent with the model of S(IV) depletion. At the lower inlet concentration of 21 ppm, the data do not fall on the model curve at S(IV) concentrations below 0.1 mM. These deviations result from the experimental uncertainty in the S(IV) concentration measurements at low S(IV). For example, if the iodometric analysis yielded an S(IV) concentration of 0.07 mM, the actual value could be 0.03 mM due to the analysis procedure not being as accurate at low S(IV) concentrations. Also, at the lower concentrations, there could be less S(IV) at the interface than perceived due to oxidation by residual oxygen in the inlet gas. Up to 5 ppm oxygen may be present in the "pure" nitrogen.

Figure 9-1 shows that there is only a very small range (depicted by curvature) where the chlorine flux should be limited by the kinetics of the Cl_2/S(IV) reaction. Looking at the 265 ppm curve, the range of kinetics-limited data would be from 0.8 to 1.2 mM S(IV). For the 21 ppm inlet, the range is from 0.07 to 0.1 mM S(IV). Thus, it is hard to extract a rate constant from the data since most of the data falls in a region where the chlorine absorption is not limited by kinetics.

Even though it was difficult to obtain a precise value for the rate constant because of the mass transfer limitations of the reactor, an approximate value can be determined. Model curves were calculated for various rate constants to see what value fitted the data best. Instead of plotting flux as a function of bulk S(IV) as was done in Figure 9-1, plotting chlorine penetration ($Cl_{2,out}/Cl_{2,in}$) as a function of $[S(IV)]_b/P_{Cl2,in}$ allows the errors in the data to be magnified. This allows better observation of which value for $k_{2,S(IV)}$ fits the data the best. Figure 9-2 plots the same data, without separately labeling the points with oxygen, and uses the same model as in Figure 9-1. The points on the y-axis (at a value of 0.5 M/atm) are actually in 0 mM S(IV). These values are plotted on the y-axis since a value of zero cannot be shown on a log-log plot.

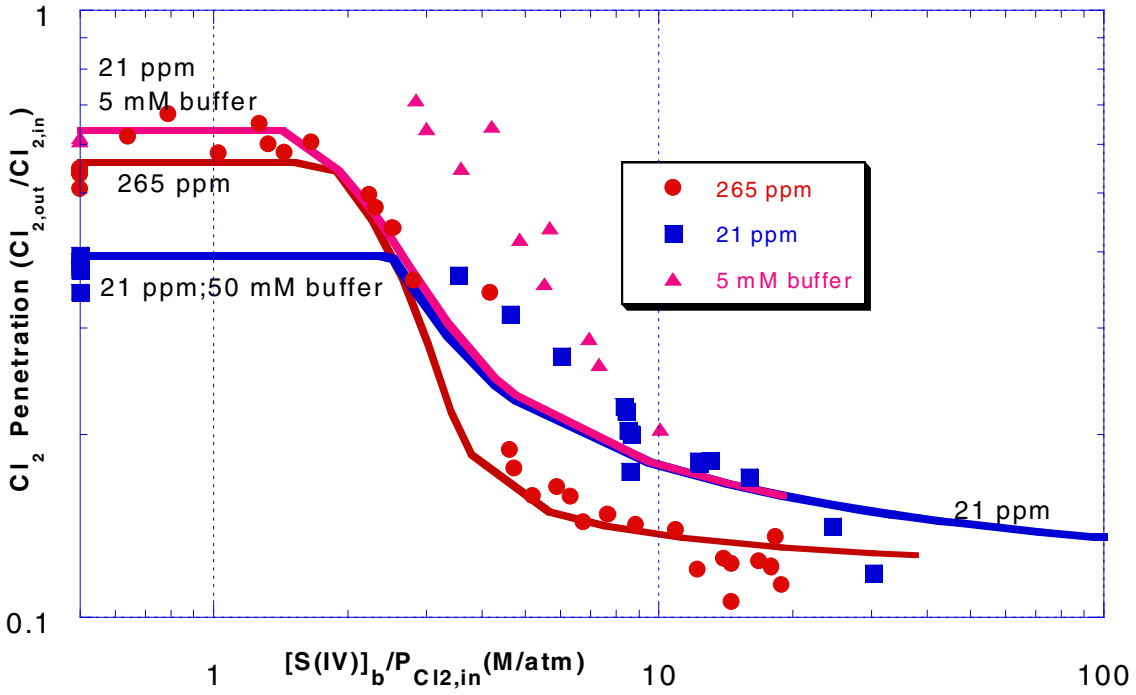

Figure 9-2. Chlorine penetration in buffered S(IV), $k_{2,S(IV)} = 2 \times 10^9$ L/mol-s

Figure 9-2 shows the same trends as Figure 9-1. The chlorine penetration is the greatest when the chlorine absorption is controlled by the buffer rate and the least when it is controlled by gas film resistance. Figures 9-2, 9-3 and 9-4 plot the same data but use different values for $k_{2,S(IV)}$. For all of these figures, the points on the y-axis represent points with no S(IV). The model curve in Figure 9-3 is calculated using an infinite rate constant while the curve in Figure 9-4 uses a lower rate constant of 2.5×10^8 L/mol-s. Figure 9-3 shows that the Cl_2/S(IV) reaction rate is not instantaneous since much of the data lie above the model curve. This instantaneous reaction model predicts a greater rate of chlorine reaction than what the data show. On the other hand, the rate constant used in Figure 9-4 is too low. The penetration is overpredicted in most of the data, signifying greater chlorine removal than what is predicted from the model.

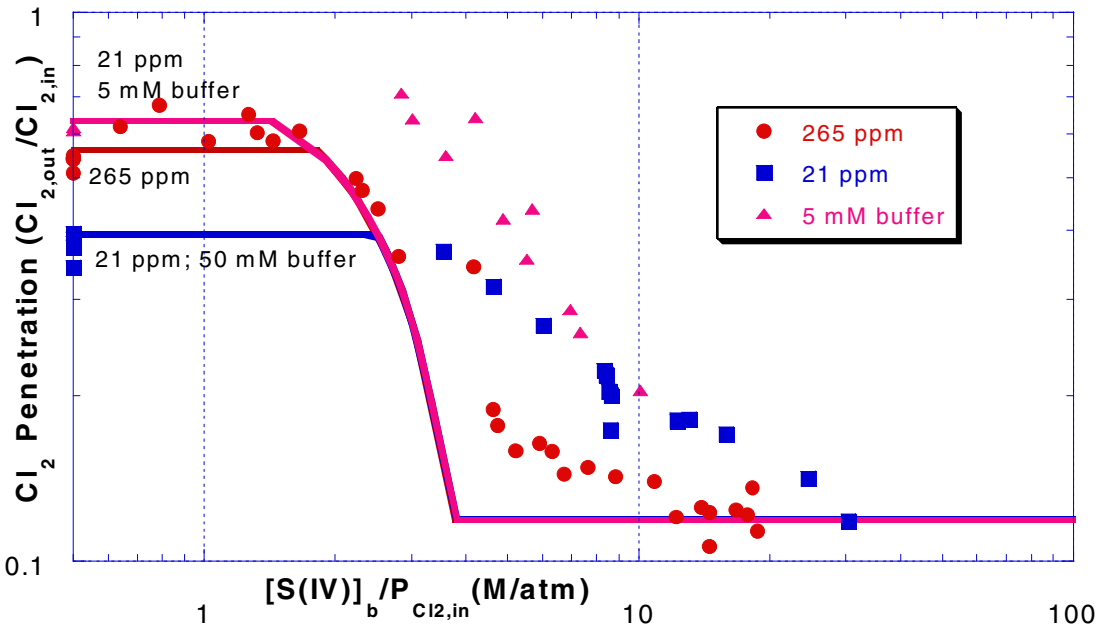

Figure 9-3. Chlorine penetration in buffered S(IV), $k_{2,S(IV)} = \infty$

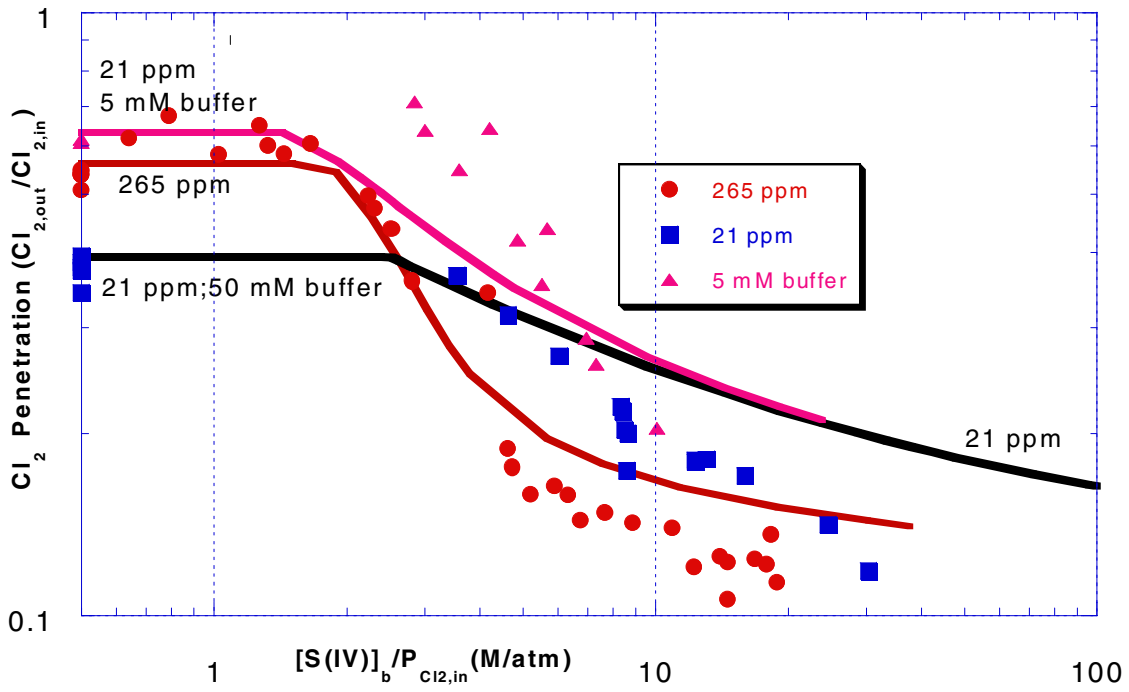

Figure 9-4. Chlorine penetration in buffered S(IV), $k_{2,S(IV)} = 2.5 \times 10^8$ L/mol-s

Therefore, the most probable value of the rate constant is 2×10^9 L/mol-s, although it could be an order of magnitude smaller or larger. However, many of the low S(IV) points, especially for the 21 ppm data, do not fall on the curve, but that could be due to the inability to accurately measure low S(IV) concentrations. In order to get a more precise rate constant, an apparatus with higher mass transfer coefficients is needed so that

the absorption falls in a region controlled by reaction kinetics instead of being controlled by mass transfer.

9.2 Chlorine absorption as a function of agitation rates

In order to further investigate if it was possible to obtain a precise rate constant in the stirred cell reactor, experiments were done in which the mass transfer coefficients were varied by varying the agitation rates (n_g and n_L). These data are listed in Table 8-13. For fast reactions that are controlled by kinetics, absorption should not be affected by changes in mass transfer coefficients. Therefore, if varying the agitation rates changes the flux of chlorine (signifying that the chlorine absorption depends on the mass transfer coefficient), kinetics cannot be extracted since mass transfer is being measured instead of kinetics. To analyze the data, the variation of flux with n_L was investigated.

Table 9-2. Flux variance with liquid agitation rate

	n_g (rpm)	n_L (rpm)	$Cl_{2,in}$(ppm)	$Cl_{2,out}$(ppm)	N_{Cl2}(kmol/m^{2}s)	d(ln N_{Cl2}/ln n_L)
A1	720	780	21.2	5.91	1.54E-09	0.600
A1	720	472	21.2	9.87	1.14E-09	
A1	720	472	21.2	10.8	1.05E-09	0.504
A1	720	898	21.2	6.82	1.45E-09	0.078
A1	720	1029	21.2	6.67	1.47E-09	
A1	1007	1039	21.2	7.74	1.36E-09	1.31
A1	752	757	21.2	12.3	8.97E-10	
A2	752	757	21.2	5.91	1.54E-09	0.131
A2	745	1053	21.2	5.23	1.61E-09	
A2	382	1063	21.2	6.06	1.53E-09	0.630
A2	382	330	21.2	13.9	7.30E-10	
A2	926	319	21.2	14.8	6.44E-10	0.626
A2	926	695	21.2	10.8	1.05E-09	0.624
A2	926	1051	21.2	7.74	1.36E-09	1.17
A2	1051	757	21.2	12.0	9.25E-10	
B1	344	713	21.2	10.5	1.08E-09	0.903
B1	332	402	21.2	14.8	6.44E-10	
B1	332	402	21.2	15.1	6.16E-10	0.618
B1	330	1044	21.2	10.2	1.11E-09	
B1	974	1058	21.2	11.4	9.88E-10	1.23
B1	749	762	21.2	14.6	6.60E-10	0.314
B1	748	408	21.2	15.8	5.42E-10	0.236
B1	749	1057	21.2	14.4	6.78E-10	
B1	1140	1083	21.2	14.8	6.47E-10	0.598
B1	1153	722	21.2	16.1	5.08E-10	
B3	1054	715	21.2	4.38	1.70E-09	0.379
B3	1069	341	21.2	8.48	1.28E-09	
B3	478	336	21.2	9.24	1.20E-09	0.274
B3	467	990	21.2	5.14	1.62E-09	
B3	720	1009	21.2	4.75	1.66E-09	0.304
B3	715	731	21.2	6.28	1.50E-09	

(Continued)

Table 9-2. Continued

	n_g (rpm)	n_L (rpm)	$Cl_{2,in}$(ppm)	$Cl_{2,out}$(ppm)	N_{Cl2}(kmol/m^2s)	d(ln N_{Cl2}/ln n_L)
B4	715	731	21.2	2.91	1.85E-09	0.014
B4	711	408	21.2	3.06	1.83E-09	
B4	369	403	21.2	4.10	1.72E-09	0.008
B4	366	938	21.2	3.98	1.74E-09	
B4	1100	946	21.2	2.42	1.89E-09	0.007
B4	1113	383	21.2	2.54	1.88E-09	0.005
B4	1117	713	21.2	2.48	1.89E-09	

From the first set of points in Table 9-2, when n_L was lowered from 780 rpm to 472 rpm, the flux changed by a factor of $n_L^{0.6}$. Based on the experiments to obtain the liquid film mass transfer coefficient of the reactor, $k^o_{L,Cl2}$ should be proportional to $n_L^{0.56}$. Since the flux depends on n_L, the rate of S(IV) diffusion to the interface (which is controlled by the liquid film mass transfer coefficient) is limiting the rate of chlorine absorption. For the points in Series A1, A2, and B1, the flux changes as n_L changes. For the points in Series B3, the overall dependence is less than the dependence in the above series, but there is still a dependence on n_L. For Series B4, the flux does not depend on the liquid agitation rate. Therefore, the flux is not being limited by S(IV) depletion at the interface.

Figure 9-5 was plotted to check if Series B4 was limited by the diffusion of chlorine to the interface, which is controlled by the gas film mass transfer coefficient, k_g. If the chlorine absorption were limited by k_g, the data in B4 would fall on a straight line corresponding to k_g.

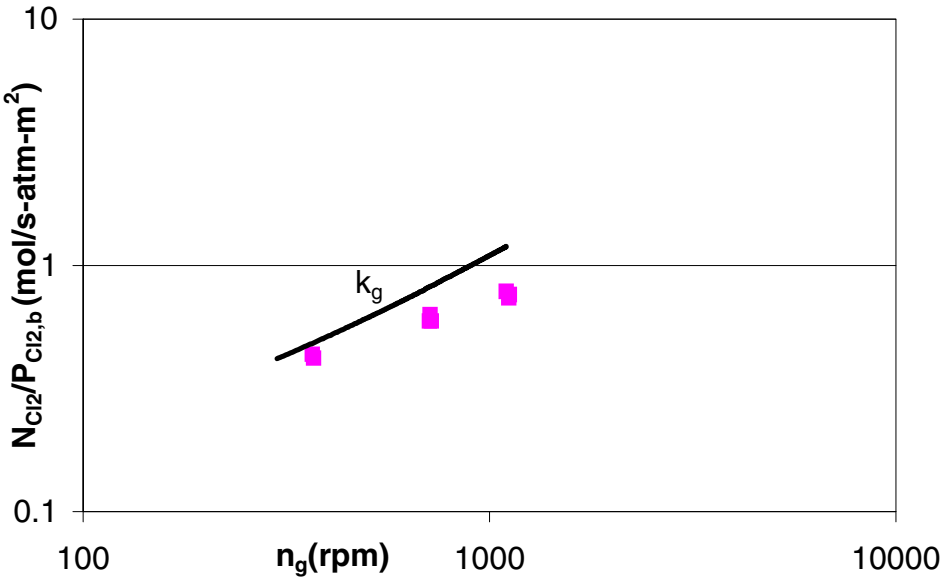

Figure 9-5. Data (Table 9-2 Series B4) limited by gas film mass transfer coefficient

Figure 9-5 shows that the points in Series B4 are close to the k_g line. Since there is a dependence on n_g, kinetics cannot be extracted since these points are dependent on k_g. Thus, there may be a very small region in between the S(IV) concentrations represented

in Series B3 and B4 for kinetics to limit the chlorine absorption. But in most of the data, chlorine absorption is not being controlled by kinetics.

9.3 Effect of succinate buffer on chlorine absorption

Table 8-11 tabulates the data obtained from varying buffer concentration, and these data are shown in Figures 9-6 and 9-7. Figures 9-6 and 9-7 show that the flux of chlorine increases as the total succinate buffer concentration increases. The maximum flux resulting from complete gas film control (corresponding to a fraction gas film resistance of one) is plotted as a line. These results show that the succinate buffer does enhance chlorine absorption. In the beginning of each series when the chlorine was run through water, there was an initial "dip" in the flux before it stabilized at the higher value. This "dip" is reflected in the graphs by the lower flux in water (0 mM buffer). The multiple data at a given $[succinate]_T$ in Figure 9-6 represent data from two experiments as shown in Table 8-11 Series B and C. The multiple data in Figure 9-7 represent the slight drift in flux that occurred with time. The rate constant, $k_{2,buf}$, was extracted from the data and found to have a slight dependence on the chlorine concentration. At the chlorine inlet concentration of 265 ppm, $k_{2,buf}$ = 29,000 L/mol-s; at inlet of 21 ppm, $k_{2,buf}$ = 149,000 L/mol-s. These values were used in the model calculations.

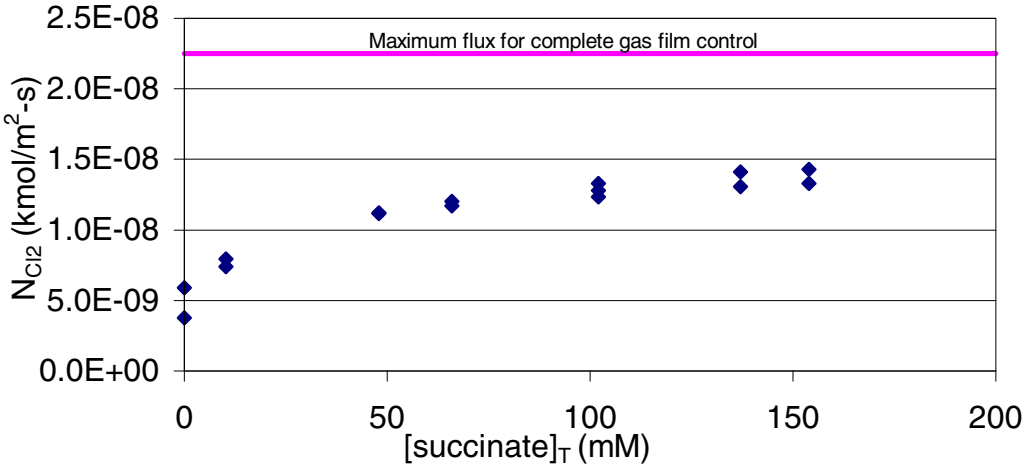

Figure 9-6. Chlorine absorption in succinate buffer with chlorine inlet of 264 ppm

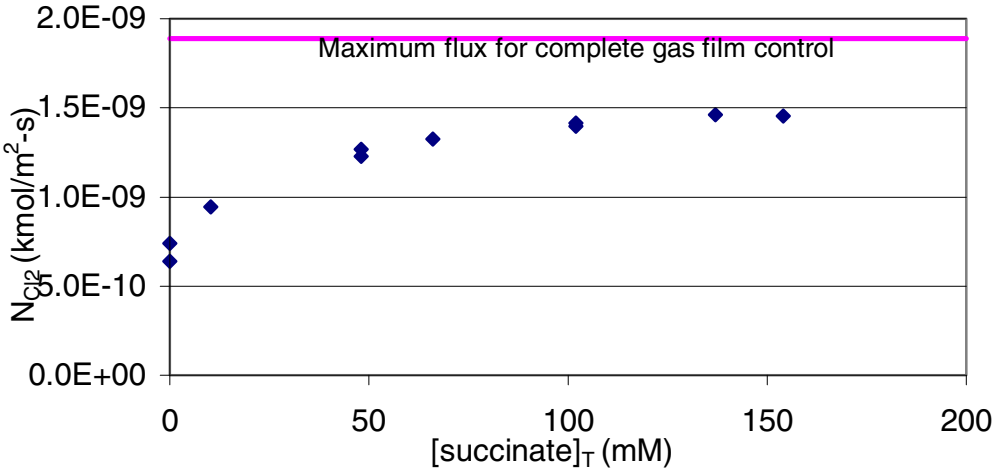

Figure 9-7. Chlorine absorption in succinate buffer with chlorine inlet of 21 ppm

There is a very narrow range for S(IV) data to determine kinetics since the chlorine flux in the 50 mM buffer is not that far from the maximum flux which is controlled by the mass transfer in the gas phase. Therefore, later experiments were done in 5 mM buffer.

9.4 S(IV) oxidation by chlorine and oxygen

Chlorine and oxygen both oxidize S(IV) to sulfate, S(VI). Several experiments were performed which established that Cl_2 is not a catalyst for the oxidation of S(IV) by oxygen. Figures 9-8 and 9-9 show how the oxidation of S(IV) depends on oxygen and chlorine. The different symbols represent each series of experiments. The dashed lines represent experiments in which chlorine and oxygen are simultaneously absorbed. The values associated with each line represent the S(IV) oxidation rate for that series. The chlorine absorption data are from Table 8-8, and the oxygen absorption data are from Table 8-9. Most of the data in Table 8-8 were at high S(IV) concentrations since it is easier to observe S(IV) oxidation when the chlorine flux is constant due to complete gas film control.

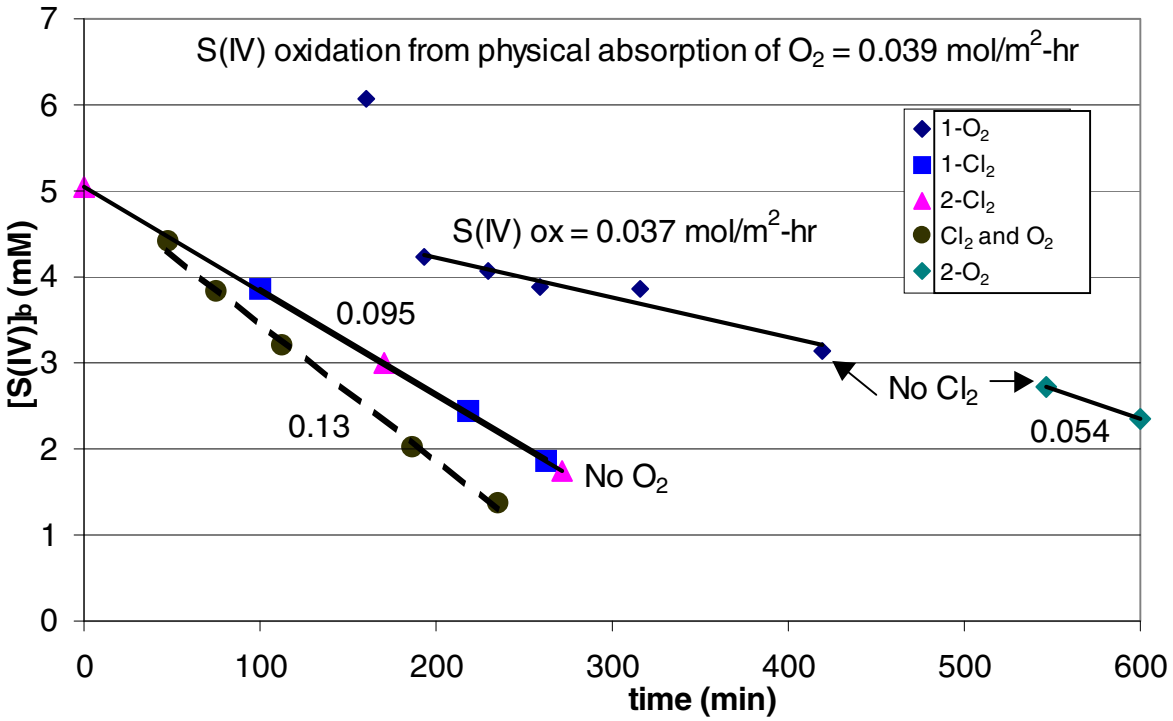

Figure 9-8. S(IV) oxidation by 275 ppm chlorine and 14.5% oxygen

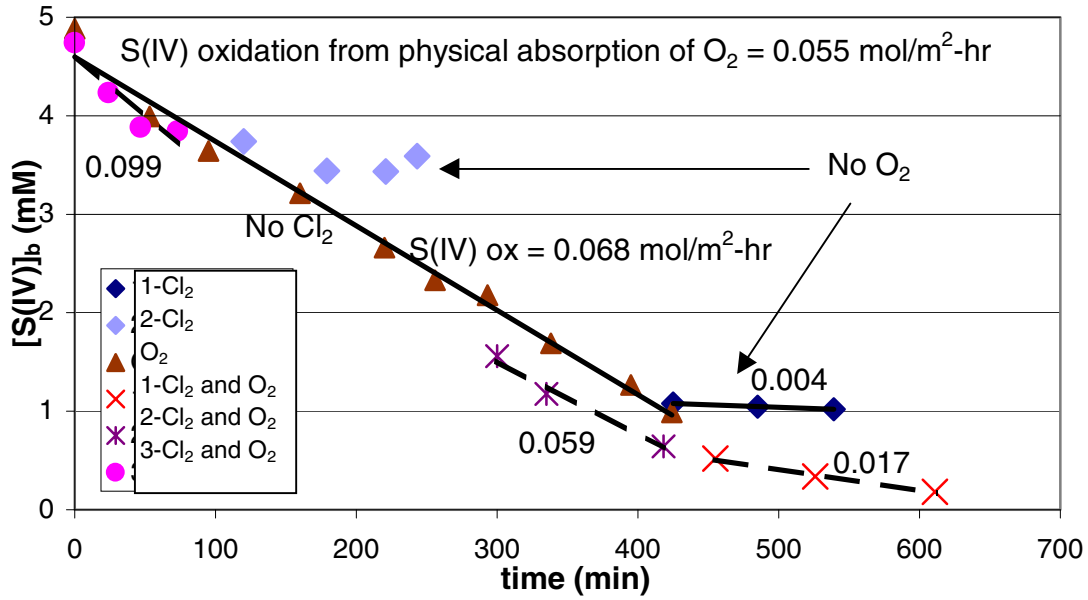

Figure 9-9. S(IV) oxidation by 21 ppm chlorine and 20.5% oxygen

Figure 9-8 shows that the effects of chlorine and oxygen on S(IV) oxidation may be additive when the inlet concentration is 275 ppm. For the points with no chlorine, the first point at 6 mM was not used in the regression since the point seemed to deviate greatly from the rest. When only oxygen is absorbed into S(IV), the S(IV) oxidation corresponds to the oxidation rate resulting from the physical absorption of 14.5 %

oxygen, which is 0.039 mol/m^2-hr. The S(IV) oxidation is calculated from the depletion rate of S(IV) observed over time. When only chlorine is absorbed, the oxidation of S(IV) is 0.095 mol/m^2-hr. There were two separate data series for these, and both data sets fell on the same line, resulting in the same S(IV) oxidation rate of 0.095 mol/m^2-hr. When chlorine and oxygen are absorbed (corresponding to S(IV) oxidation rate of 0.13 mol/m^2-hr), about three-fourths of the S(IV) oxidation is due to the reaction of chlorine with S(IV). In this case, the chlorine does not seem to be catalyzing S(IV) oxidation since the S(IV) oxidation seems to be additive.

Figure 9-9 shows data in which the chlorine inlet concentration is significantly lower at 21 ppm. In this case, the oxidation of S(IV) due to reaction with chlorine (Series 1-Cl_2 and 2-Cl_2) is practically negligible. Physical absorption of 20.5% oxygen corresponds to S(IV) oxidation of 0.055 mol/m^2-hr. Thus, the oxidation of S(IV) without chlorine (Series O_2) is in the range of oxidation due to physical absorption of O_2. It should be noted that in the data in Series O_2, the last four points contained 0.025 mM Fe^{+2}. Fe^{+2} was added in order to enhance oxygen absorption since ferrous ion is a well-known catalyst. However, Figure 9-9 shows that adding ferrous ion did not enhance oxygen absorption (since the S(IV) oxidation rate in Series O_2 did not change after Fe^{+2} addition).

At very low S(IV) concentrations (< 0.5 mM), the S(IV) oxidation is much less (0.017 mol/m^2-hr) than that expected from physical absorption of oxygen. This may occur because at these low concentrations, there is barely any S(IV) at the interface. When S(IV) is between 0.5 and 1.5 mM (Series 2-Cl_2 and O_2), it seems that the S(IV) oxidation is equivalent to that which would result from the physical absorption of oxygen. Thus, chlorine does not seem to enhance S(IV) oxidation in this case. At high S(IV) concentrations (around 4 mM), the slope of the line for Series 3-Cl_2 and O_2 is steeper, and the S(IV) oxidation is much greater at 0.099 mol/m^2-hr. Chlorine may be catalyzing S(IV) oxidation, but it is hard to tell from looking at the figure. More data would need to be taken in this range.

9.5 Discussion of electrochemical analyzer data

The discussion so far has only dealt with data from the IMS analyzer. Figure 9-10 overlays the electrochemical data from Tables 8-6 and 8-7 with the IMS data in Figure 9-1. Tables 8-6 and 8-7 only include data after the calibration of the electrochemical analyzer was improved.

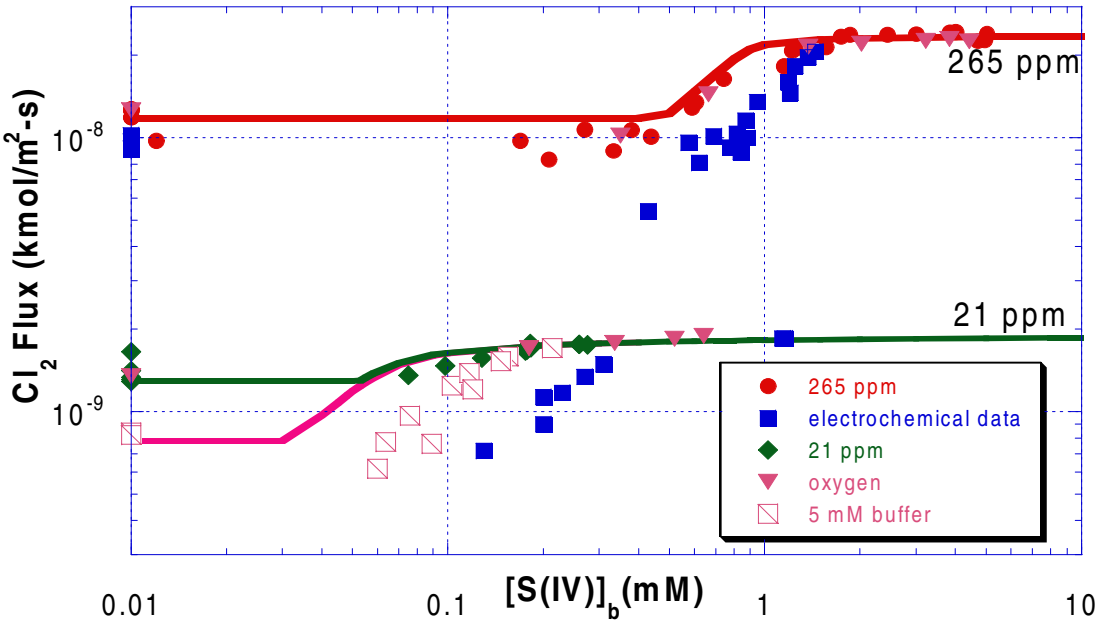

Figure 9-10. Electrochemical analyzer data overlaid onto IMS data

The trends are similar, but the data from the electrochemical analyzer do not fit the model. The data obtained using the electrochemical analyzer are at a slightly lower k_L^o value of 2.3 x 10^{-5} m/s, while the model curves were calculated using the k_L^o value of 2.45 x 10^{-5} m/s (since this was the value for the data taken with the IMS analyzer). Even if the lower k_L^o value was used in the above model calculations, the electrochemical analyzer data would not fit the model. In order for the data to fit the model, the liquid film mass transfer coefficient used in the model would need to be approximately 1.23 x 10^{-5} m/s.

Figure 9-11 shows the above electrochemical data in a separate figure to better see trends. As expected, the percent gas film resistance increases (signifying enhanced reaction) as S(IV) increases until 100% gas film control is reached. Figure 9-11 also shows that at the low chlorine concentration, the absorption is more likely to approach gas film control at lower S(IV) concentrations. This is expected since at lower chlorine concentrations, it takes less S(IV) to react completely with the chlorine. Figure 9-11 also shows that the point at 0.43 mM S(IV) seems to have a lower reaction rate than the points with no S(IV). This is equivalent to the S(IV) inhibition seen with the IMS data.

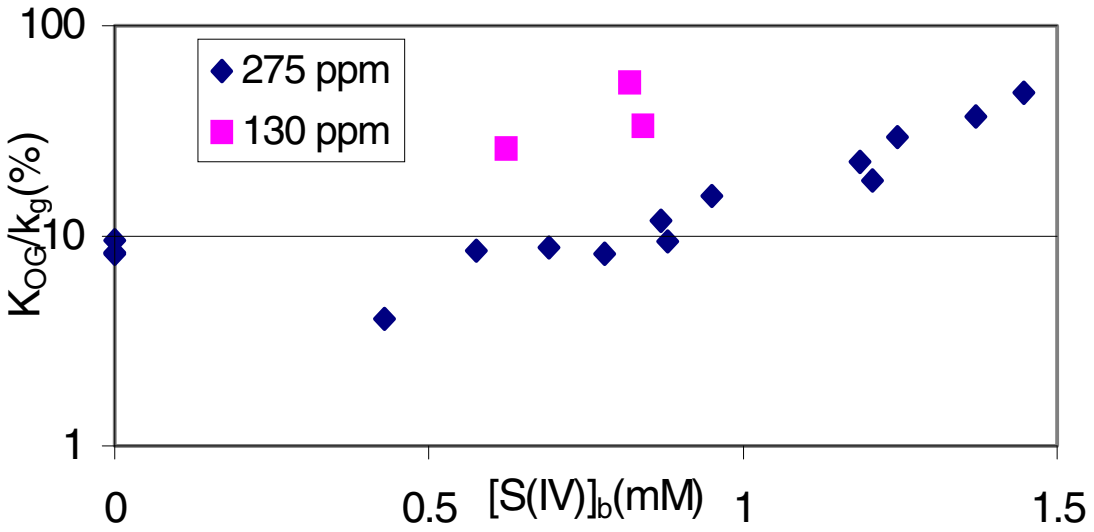

Figure 9-11. Chlorine absorption in 0 – 2 mM S(IV) in 50 mM buffer using electrochemical analyzer

Figure 9-12 shows that the flux of chlorine is linear with bulk S(IV), signifying a region controlled by S(IV) diffusion to the interface.

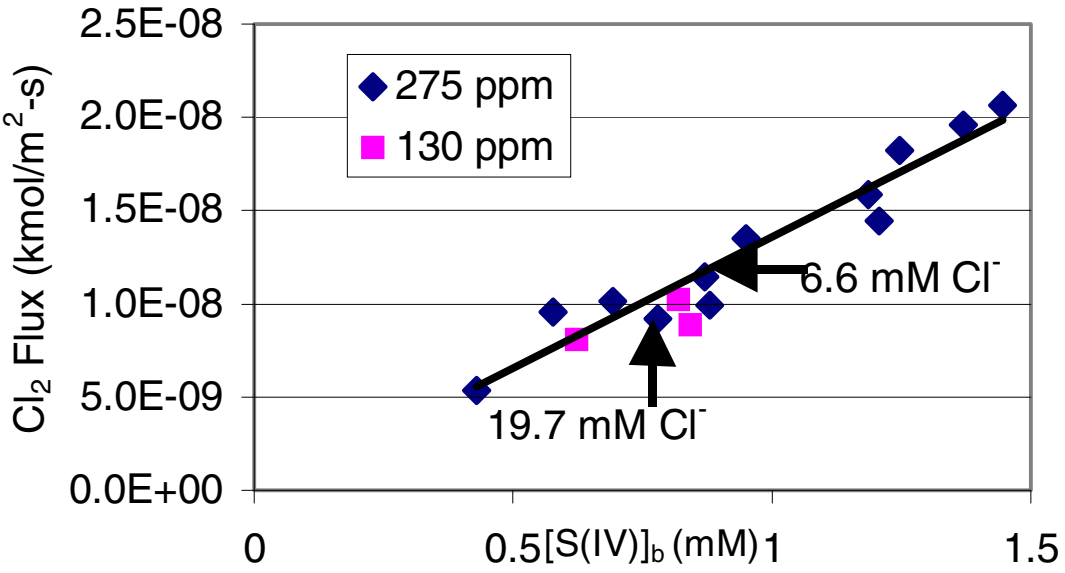

Figure 9-12. Effect of chloride seen from data obtained using electrochemical analyzer

Figure 9-12 also shows that chloride (up to 20 mM) has no effect on the rate of chlorine absorption in S(IV). The two marked points have increased levels of chloride (stock solution of NaCl was added to reactor). The other points have chloride concentrations resulting from only chlorine absorbing to form chloride (no external addition of chloride). The chloride concentrations for these points range from 0.1 to 2 mM. The chloride does

not seem to have any effect on the chlorine absorption since the two points with elevated chlorine seem to follow the trend of the other points. Thus, at chloride concentrations less than 0.02 M, there is no effect on the chlorine reaction with S(IV). This makes sense since chloride should not affect the Cl_2/S(IV) reaction if the reaction is irreversible.

Even the earlier electrochemical analyzer data (prior to data in Table 8-6) show that S(IV) enhances chlorine absorption. However, these data cannot be rigorously analyzed because of the analyzer problems mentioned earlier. Table 8-1 does show that pure sulfite (which is at a higher pH than the buffered S(IV) solutions) may enhance absorption more than the buffered S(IV) solutions. For the pH 7-8.5 data, the reaction rate is so fast that the system is essentially gas film controlled.

9.6 Mercury removal in a typical limestone slurry scrubber

The expected mercury removal in a limestone slurry scrubber can be predicted using the extracted rate constant for the Cl_2/S(IV) reaction, a preliminary rate constant for Hg/Cl_2 (Zhao and Rochelle, 1999), and typical mass transfer characteristics for a scrubber. Table 9-3 tabulates the parameters used in the model. The value for $k_{2,S(IV)}$ at 55°C was estimated from the value at 25°C. The model must be supplied with a given chlorine inlet and a constant S(IV) concentration. The model accounts for the two simultaneous reactions occurring at the gas/liquid interface: the depletion of chlorine through reaction with S(IV) ($k_{2,S(IV)}$) and the reaction of elemental mercury with chlorine ($k_{2,Hg}$).

Table 9-3. Parameters used to predict mercury removal

	25°C	55°C
$k_{2,S(IV)}$ (L/mol-s)	2×10^{9}	2×10^{11}
$k_{2,Hg}$ (L/mol-s)	1.7×10^{15}	1.4×10^{17}
k_g (kmol/s-atm-m^2)	0.001	0.001
D_{Cl_2} (m^2/s)	1.48×10^{-9}	2.15×10^{-9}
D_{Hg} (m^2/s)	1.19×10^{-9}	2.21×10^{-9}
H_{Hg} (atm-m^3/kmol)	8.91	35.64

In a limestone slurry scrubber, chlorine absorption will be gas film controlled. Thus, Equation 5-8 can be used to calculate the flux of chlorine. The bulk chlorine in the scrubber depends on the number of gas phase mass transfer units (N_g), which is defined as k_gA/G. Equation 9-7 shows this dependence. The total number of gas phase mass transfer units in a typical scrubber is 6.9.

$$P_{Cl_2,b} = P_{Cl_2,in}\exp\left(-N_g\right) \tag{9-7}$$

The chlorine flux calculated from Equation 5-8 must equal the flux from Equation 5-4, thus allowing the concentration of chlorine at the interface to be determined when the S(IV) concentration is provided. The interfacial chlorine concentration is very important in predicting mercury absorption.

To predict mercury absorption due to reaction with chlorine, an expression similar to Equation 5-4 is used. The enhancement of mercury removal is:

$$E_{Hg} k_L^o = \sqrt{D_{Hg} k_{2,Hg} [Cl_2]_i} \tag{9-8}$$

The rate at which mercury is absorbed is the product of the driving force (y_{Hg}) and the overall gas phase mass transfer coefficient (K_{OG}) given in Equation 5-10. Thus, the rate of mercury absorption in a scrubber is given by Equation 9-9:

$$-G dy_{Hg} = y_{Hg} \frac{k_g}{1 + \frac{k_g H_{Hg}}{k_L^o E_{Hg}}} dA \tag{9-9}$$

Substituting N_g for $k_g A/G$ and integrating:

$$\int_{y_{Hg,in}}^{y_{Hg}} \frac{dy_{Hg}}{y_{Hg}} = -\int_0^{6.9} \frac{1}{1 + \frac{k_g H_{Hg}}{k_L^o E_{Hg}}} dN_g \tag{9-10}$$

Equation 9-10 was used to quantify mercury removal. Tables 9-4 and 9-5 and Figure 9-13 show the mercury penetration (Hg_{out}/Hg_{in}) as a result of chlorine injection to the scrubber. The model curves were calculated at constant S(IV) concentrations of 1 and 10 mM.

Table 9-4. Mercury penetration in limestone slurry scrubber at 25°C

$Cl_{2,in}$(ppm)	1 mM S(IV)	10 mM S(IV)
0.1	0.0249	0.0554
1	0.0057	0.0114
10	0.0021	0.0032

Table 9-5. Mercury penetration in limestone slurry scrubber at 55°C

$Cl_{2,in}$(ppm)	1 mM S(IV)	10 mM S(IV)
0.1	0.0293	0.0649
1	0.0065	0.0133
10	0.0023	0.0036

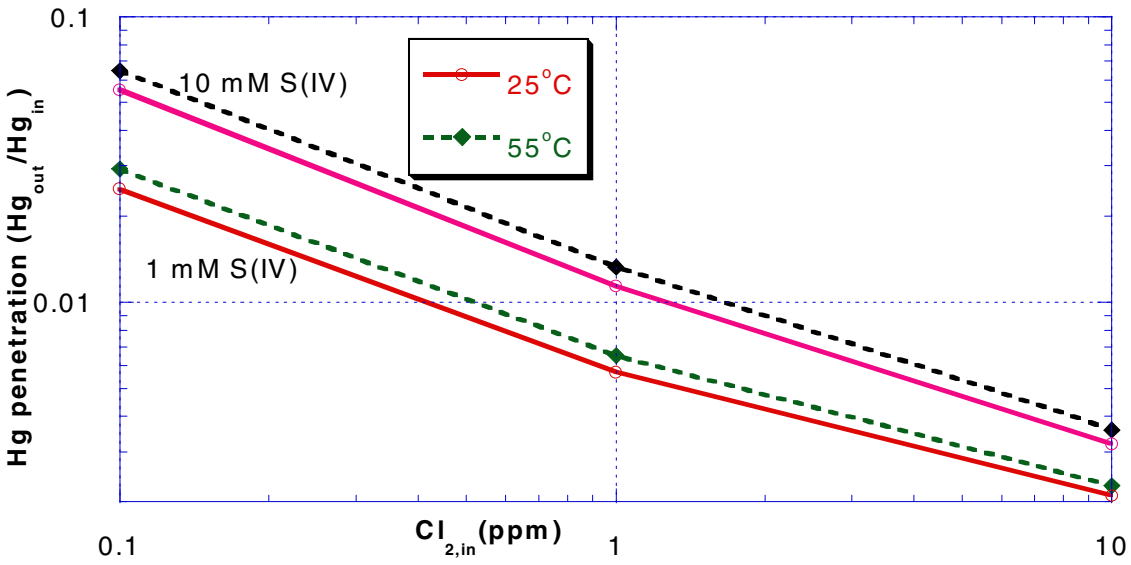

Figure 9-13. Predicted mercury penetration

Mercury removal increases (penetration decreases) as the chlorine injected increases. Mercury removal decreases as S(IV) increases due to greater depletion of chlorine at the interface. At the higher temperature, there is less chlorine at the interface due to the higher reaction rate of chlorine with S(IV). However, since the reaction rate of mercury and chlorine also increases with temperature, significant mercury removal still occurs. Based on this model, only 1 ppm chlorine is needed to obtain 99 % mercury removal. Since chlorine absorption is gas film controlled, 99.9% chlorine removal will be achieved due to reaction with S(IV).

References

Ashour, S.S., E.B. Rinker, and O.C. Sandall, "Absorption of Chlorine into Aqueous Bicarbonate Solutions and into Aqueous Hydroxide Solutions," AIChE J., 42(3), 671-682 (1996).

Askew, W. C., and S. J. Morisani, "Determining Chlorine Concentrations in Air and Water Samples for Scrubbing Studies Using Ion Chromatography," J. Chromatogr. Sci., 27, 42-46 (1989).

Brian, P.L.T., J.E. Vivian, and C. Piazza, "The Effect of Temperature on the Rate of Absorption of Chlorine into Water," Chem. Eng. Sci., 21, 551-558 (1966).

Chang, C.S., "Mass Transfer with Equilibrium Chemical Reaction, Sulfur Dioxide Absorption in Aqueous Solutions," Ph.D. dissertation, The University of Texas at Austin, December 1979.

Critchfield, J.E., "CO_2 Absorption/Desorption in Methyldiethanolamine Solutions Promoted with Monoethanolamine and Diethanolamine: Mass Transfer and Reaction Kinetics," Ph.D. Dissertation, The University of Texas at Austin, 1988.

Danckwerts, P.V., Gas-Liquid Reactions, McGraw-Hill Book Co., New York, NY (1970).

Dutchuk, M.J., "Nitrogen Dioxide Absorption in Aqueous Dithionite," M.S. Thesis, The University of Texas at Austin, May 1999.

Ernst, W.R., B. Indu, and M.F. Hoq, "Influence of Mercuric Nitrate on Species and Reactions Related to Chlorine Dioxide Formation," Ind. Eng. Chem. Res., 36, 11-16 (1997).

Fedorovskaya, L.F., V.A. Skripnik, L.I. Kravetskii, and I.M. Umanskaya, "Mechanism and Kinetics of Mercury Oxidation by Chlorine-Containing Solutions," Translated from Zhurnal Prikladnoi Khimii, 52(6), 1233-1237 (1979).

Fogelman, K.D., D.M. Walker, and D.W. Margerum, "Non-metal Redox Kinetics: Hypochlorite and Hypochlorous Acid Reactions with Sulfite," Inorg. Chem., 28, 986-993 (1989).

Gordon, G., B. Slootmaekers, S. Tachiyashiki, and D. Wood, "Minimizing Chlorite Ion and Chlorate Ion in Water Treated with Chlorine Dioxide," Amer. Water Works Assoc. J., 82, 160-165 (1990).

Hall, B.B., "An Experimental Study of Mercury Reactions in Combustion Flue Gases," Ph.D. dissertation, Goteborgs Universitet (Sweden), 1992.

Keating, M.H., K.R. Mahaffey, R. Schoeny, G.E. Rice, and O.R. Bullock, "Executive Summary," Mercury Study Report to Congress (1), EPA/452/R-97-003 (NTIS

PB 98-124738), U.S. Environmental Protection Agency, Office of Air Quality Planning and Standards, Research Triangle Park, NC, December 1997.

Kolthoff, I.M., and R. Belcher, Volumetric Analysis, Volume III, 199-374, Interscience Publishers, Inc., New York, NY (1957).

Jensen, J.S., and G. R. Helz, "Rates of Reduction of N-Chlorinated Peptides by Sulfite: Relevance to Incomplete Dechlorination of Wastewaters," Environ. Sci. Technol., 32, 516-522 (1998).

Lifshitz, A., and B. Perlmutter-Hayman, "The Kinetics of the Hydrolysis of Chlorine. III. The Reaction in the Presence of Various Bases, and a Discussion of the Mechanism," J. Phys. Chem., 66, 701-705 (1962).

Livengood, C.D., and M.H. Mendelsohn, "Improved Mercury Control in Wet Scrubbing Through Modified Speciation," presented at the EPRI-DOE-EPA Combined Utility Air Pollutant Control Symposium, Washington, D.C., August 25-29,1997.

Shen, C.H., "Nitrogen Dioxide Absorption in Aqueous Sodium Sulfite," Ph.D. dissertation, The University of Texas at Austin, May 1997.

Spalding, C.W., "Reaction Kinetics in the Absorption of Chlorine into Aqueous Media," AIChE J., 8(5), 685 (1962).

Suzuki, K., and G. Gordon, "Stoichiometry and Kinetics of the Reaction between Chlorine Dioxide and Sulfur(IV) in Basic Solutions," Inorg. Chem., 17(11), 3115-3118 (1978).

Wang, T. X., and D. W. Maregerum, "Kinetics of Reversible Chlorine Hydrolysis: Temperature Dependence and General-Acid/Base-Assisted Mechanisms," Inorg. Chem., 33, 1050-1055 (1994).

Zhao, L.L., "Mercury Absorption in Aqueous Solutions," Ph.D. dissertation, The University of Texas at Austin, May 1997.

Zhao, L.L., and G.T. Rochelle, "Mercury Absorption in Aqueous Hypochlorite," Chem. Eng Sci., 54, 655-662 (1999).

Zhao, L.L., and G.T. Rochelle, "Mercury Absorption in Aqueous Permanganate," AIChE J., 42, (1996).

Appendix A Gas film mass transfer coefficient data

Table A-1 shows the k_g values calculated using the IMS analyzer data. All of the data are for chlorine absorption in 0.28 M sodium hydroxide (NaOH).

Table A-1. Gas film mass transfer coefficient (k_g), IMS analyzer

n_g (rpm)	$Cl_{2,in}$ (ppm)	$Cl_{2,out}$ (ppm)	N_{Cl2}(kmol/m^2-s)	k_g(mol/s-atm-m^2)
750	21.2	2.47	1.89E-09	0.765
623	21.2	2.69	1.87E-09	0.694
500	21.2	3.00	1.84E-09	0.613
762	21.2	2.50	1.89E-09	0.755

Table A-2 shows the k_g values calculated using the electrochemical analyzer data. The data use the improved calibration shown in Figure 8-2, but the data were taken before the experimental modifications were made to reduce scatter.

Table A-2. Gas film mass transfer coefficient (k_g), electrochemical sensor analyzer

n_g (rpm)	$Cl_{2,in}$ (ppm)	$Cl_{2,out}$ (ppm)	N_{Cl2}(kmol/m^2-s)	k_g(mol/s-atm-m^2)
428	197	35.0	1.63E-08	0.46
357	197	37.8	1.60E-08	0.42
292	197	40.4	1.57E-08	0.39
546	197	32.2	1.65E-08	0.51
691	197	28.5	1.69E-08	0.59
514	197	34.3	1.63E-08	0.48
403	197	37.6	1.60E-08	0.43
303	197	41.5	1.56E-08	0.38
714	197	28.5	1.69E-08	0.59

Table A-3 shows the k_g values calculated using the electrochemical analyzer data after the experimental modifications were made to reduce scatter.

Table A-3. Gas film mass transfer coefficient (k_g), electrochemical analyzer after modifications to reduce scatter

n_g (rpm)	$Cl_{2,in}$ (ppm)	$Cl_{2,out}$ (ppm)	N_{Cl2}(kmol/m^2-s)	k_g(mol/s-atm-m^2)
629	195	26.2	1.69E-08	0.65
474	195	30.6	1.65E-08	0.54
352	195	34.5	1.61E-08	0.47
707	195	24.9	1.71E-08	0.69
484	195	31.6	1.64E-08	0.52
710	195	25.3	1.70E-08	0.67
710	149	19.7	1.31E-08	0.66
710	93	12.8	8.25E-09	0.65
490	93	16.5	7.87E-09	0.48
362	93	18.2	7.69E-09	0.42
711	93	12.6	8.27E-09	0.65
616	197	27.8	1.70E-08	0.61
519	197	31.7	1.66E-08	0.52
412	197	36.7	1.61E-08	0.44
330	197	41.3	1.56E-08	0.38
597	197	30.9	1.67E-08	0.54
342	197	39.8	1.58E-08	0.40
720	197	26.6	1.71E-08	0.64
428	197	36.1	1.61E-08	0.45
288	197	41.9	1.56E-08	0.37
704	197	27.0	1.71E-08	0.63

Appendix B Liquid film mass transfer coefficient data and correlations

Table B-1 lists all the data used to determine k^{o}_{L,Cl_2}. Chlorine desorption was measured from a sodium hypochlorite solution in 0.1 M HCl. These data were all obtained using the IMS analyzer.

Table B-1. Data used to determine k^{o}_{L,Cl_2} correlations

n_L(rpm)	t(min)	$Cl_{2,out}$ (ppm)	$\ln P_{Cl_2}$ (atm)
729	0	284	-8.17
	6	264	-8.24
	12	248	-8.30
	18	232	-8.37
	20.6	222	-8.41
	24	213	-8.46
	30	203	-8.50
	36	186	-8.59
	42	168	-8.69
	48	158	-8.76
	54	148	-8.82
	60	135	-8.91
	64.8	129	-8.96
	75	112	-9.10
305	0	56.7	-9.78
	6	53.8	-9.83
	12	51.2	-9.88
	18	50.2	-9.90
	25.1	47.3	-9.96
504	0	65.4	-9.63
	6	61.9	-9.69
	12	58.6	-9.74
	14.2	57.0	-9.77
	18	56.3	-9.78
	24	52.1	-9.86
734	0	66.4	-9.62
	4.2	63.5	-9.66
	12	57.0	-9.77
	18	53.4	-9.84
	24	50.5	-9.89
	32.4	45.7	-9.99
699	0	289	-8.15
	6	275	-8.20
	9.6	264	-8.24
	12	257	-8.27
	18	238	-8.34
	24	218	-8.43
	30	203	-8.50

(Continued)

Table B-1. Continued

n_L(rpm)	t(min)	$Cl_{2,out}$(ppm)	$\ln P_{Cl_2}$ (atm)
	36	186	-8.59
	42	171	-8.67
	48	156	-8.76
228	0	62.3	-9.68
	6	58.7	-9.74
	12	58.0	-9.75
	18	54.8	-9.81
	24	54.1	-9.82
	27.6	51.5	-9.87
600	0	104.0	-9.17
	3.6	98.4	-9.23
	7.2	95.8	-9.25
	9.6	91.9	-9.29
	15.6	88.7	-9.33
	21.6	84.1	-9.38
	25.2	78.6	-9.45
306	0	45.0	-10.01
	6	43.4	-10.05
	12	40.4	-10.12
	18	39.1	-10.15
	24	36.5	-10.22
514	0	54.4	-9.82
	2.4	52.8	-9.85
	8.4	49.5	-9.91
	14.4	47.3	-9.96
	20.4	44.3	-10.02
	26.4	41.1	-10.10
718	0	52.5	-9.86
	2.4	50.5	-9.89
	8.4	46.6	-9.97
	14.4	43.4	-10.05
	20.4	39.8	-10.13
	26.4	37.5	-10.19

For each n_L, a plot of $\ln P_{Cl_2}$ against time was generated, and the liquid film mass transfer coefficient was determined from the slope of the line. Table B-2 lists the k^{o}_{L,Cl_2} values obtained from the slopes of these lines.

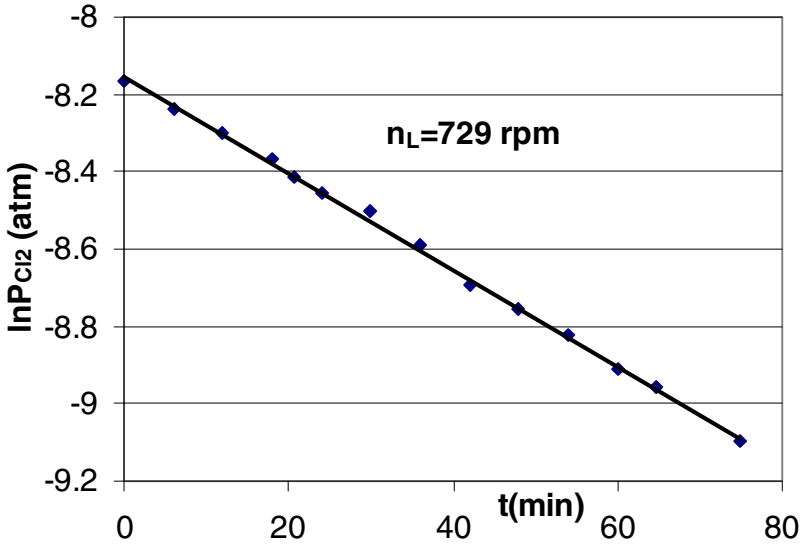

Figure B-1. Extracting $k^{o}_{L,Cl2}$ at 729 rpm

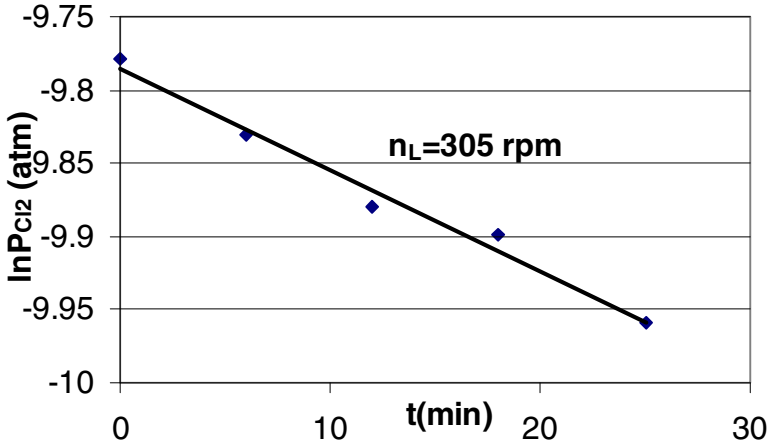

Figure B-2. Extracting $k^{o}_{L,Cl2}$ at 305 rpm

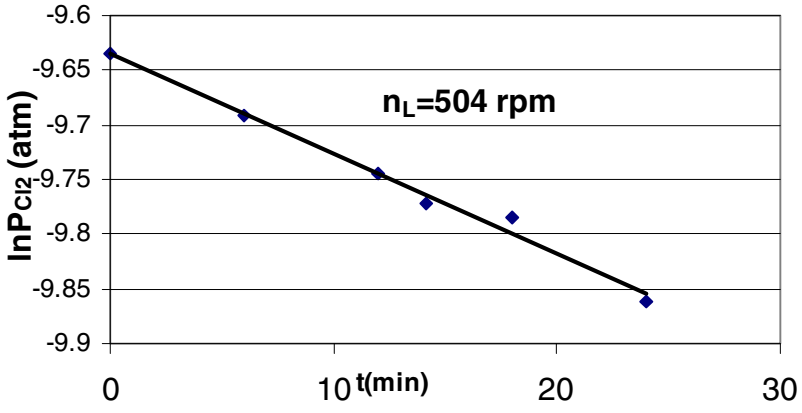

Figure B-3. Extracting $k^{o}_{L,Cl2}$ at 504 rpm

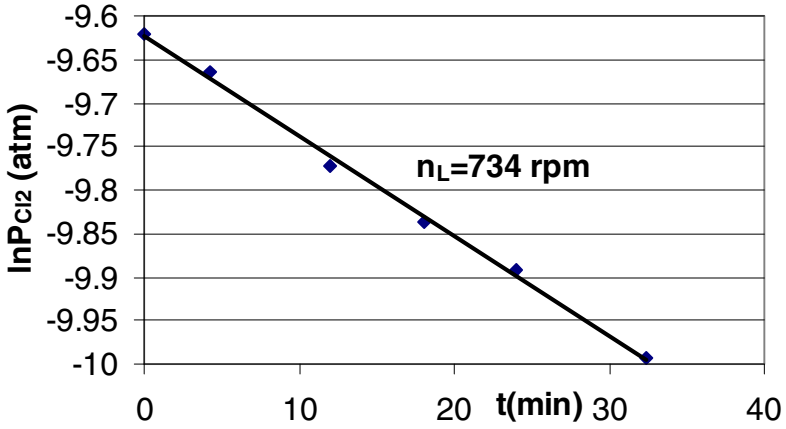

Figure B-4. Extracting $k^{o}_{L,Cl2}$ at 734 rpm

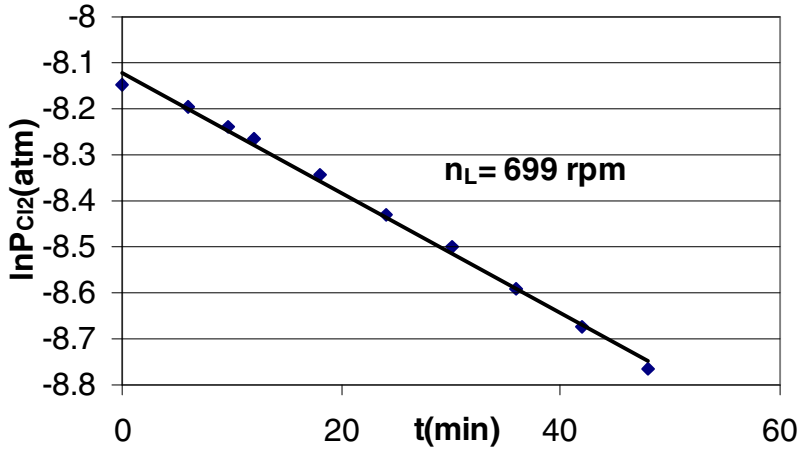

Figure B-5. Extracting $k^{o}_{L,Cl2}$ at 699 rpm

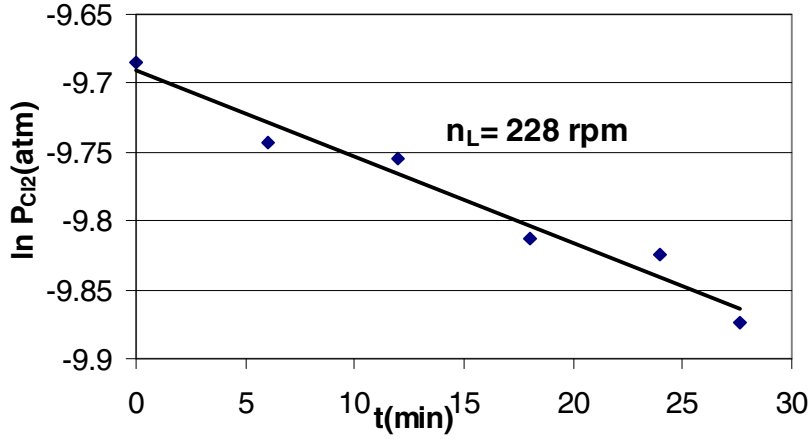

Figure B-6. Extracting $k^{o}_{L,Cl2}$ at 228 rpm

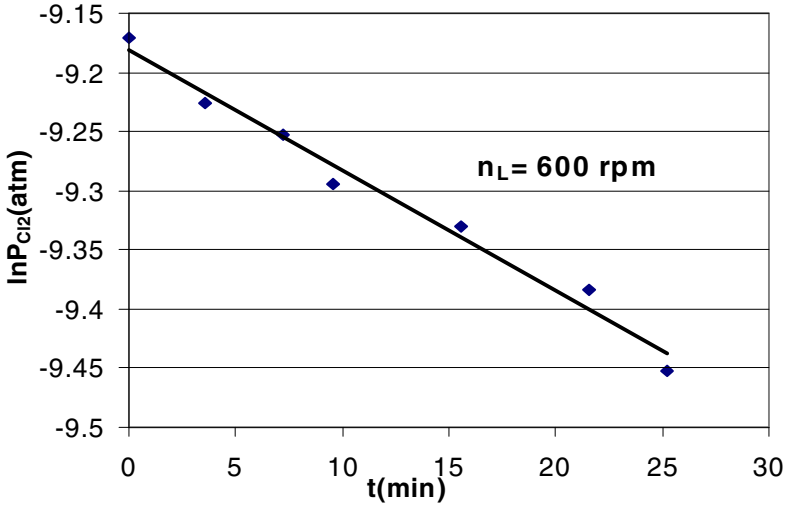

Figure B-7. Extracting $k^{o}_{L,Cl2}$ at 600 rpm

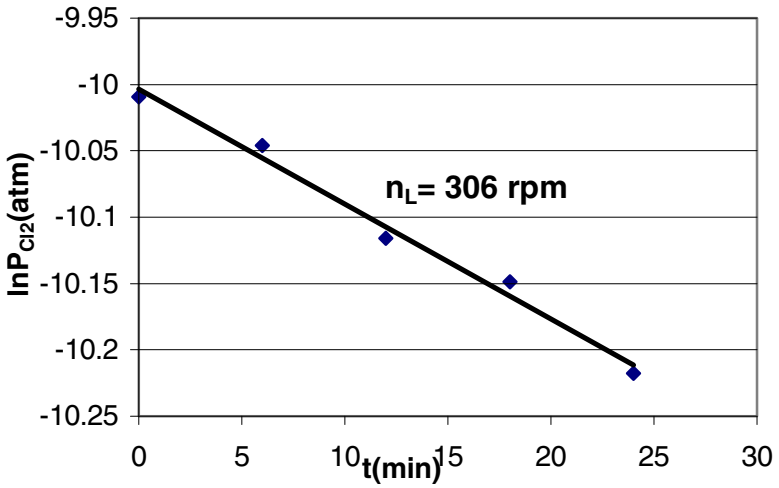

Figure B-8. Extracting $k^{o}_{L,Cl2}$ at 306 rpm

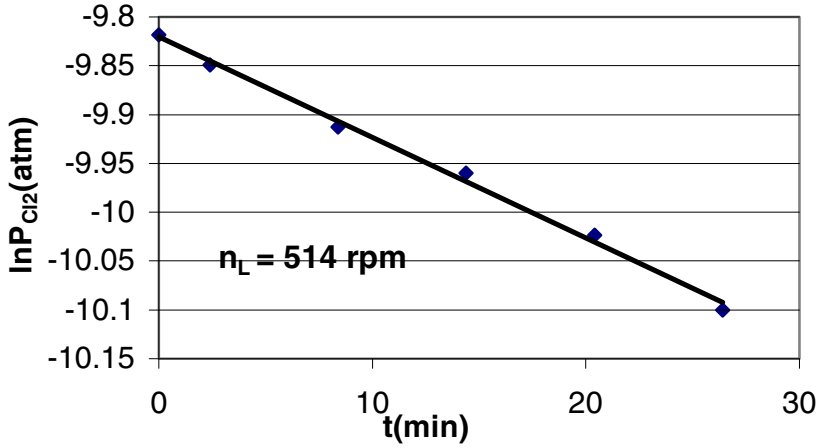

Figure B-9. Extracting $k^{o}_{L,Cl2}$ at 514 rpm

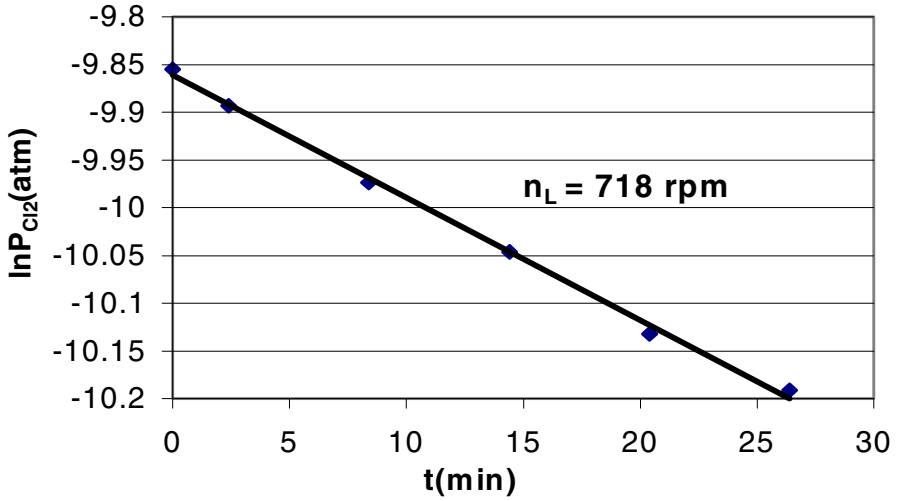

Figure B-10. Extracting $k^{o}_{L,Cl2}$ at 718 rpm

Table B-2. Physical liquid film mass transfer coefficient for chlorine

n_L(rpm)	k^{o}_{L,Cl_2} (m/s)
729	2.73E-05
305	1.51E-05
504	2.01E-05
734	2.51E-05
699	2.86E-05
228	1.37E-05
600	2.23E-05
306	1.90E-05
514	2.25E-05
718	2.80E-05